Ref. Ares(2022)1442175 - 25/02/2022

Horizon 2020 Programme

CoCliCo

Research and Innovation Action (RIA)

This project has received funding from the European Union's Horizon 2020 research and innovation programme under grant agreement No 101003598

Start date : 2021-09-01 Duration : 48 Months

State of the art and GIS layer on current vulnerability and exposure

Authors : Dr. Elco KOKS (VU Amsterdam), Elco Koks (IVM-VU), Joël De Plaen (IVM-VU), Sadhana Nirandjan (IVM-VU), Jeremy Rohmer (BRGM), Rémi Thiéblemont (BRGM), Athanasios Vafeidis (CAU), Giovanna Pisacane (ENEA), Daniel Lincke (GCF)

CoCliCo - Contract Number: 101003598

Project officer: Anna Natasa ASIK

Document title	State of the art and GIS layer on current vulnerability and exposure
Author(s)	Dr. Elco KOKS, Elco Koks (IVM-VU), Joël De Plaen (IVM-VU), Sadhana Nirandjan (IVM-VU), Jeremy Rohmer (BRGM), Rémi Thiéblemont (BRGM), Athanasios Vafeidis (CAU), Giovanna Pisacane (ENEA), Daniel Lincke (GCF)
Number of pages	50
Document type	Deliverable
Work Package	WP5
Document number	D5.1
Issued by	VU Amsterdam
Date of completion	2022-02-25 13:26:29
Dissemination level	Public

Summary

This report presents an overview of the current state-of-knowledge on exposure, vulnerability, risk and adaptation in relation to coastal flooding and the built environment. While the report has shown that there is a wealth of knowledge and data available at the start of this project, several gaps have been identified that need and will be addressed within CoCliCo. Firstly, improving the European coverage of geospatial data of critical infrastructure assets. While some infrastructure assets may have a good coverage of data availability across Europe through open-source initiatives such as OpenStreetMap (e.g., transport infrastructure), several infrastructures are also still far from complete (e.g., low-tier electricity networks). Secondly, we will make first steps in using social media and novel Natural Language Processing methods to develop a first set of vulnerability thresholds to provide a link between hazard intensity and network service functioning. This is currently mostly unknown within both a European and global context. Thirdly, development of future population exposure under different scenarios. This will provide the basis to identify how adaptation measures influence the development of population. Within CoCliCo, we hope to provide first answers. Finally, CoCliCo will make additional steps in developing a wide range of coastal adaptation measures for Europe, ranging from nature-based solutions to coastal migration. These measures will be incorporated within a risk modelling framework, allowing us to assess the potential benefits of each individual measure.

Approval

Date	By
2022-02-25 13:26:42	Dr. Elco KOKS (VU Amsterdam)
2022-02-25 14:11:43	Dr. Gonéri LE COZANNET (BRGM)

CoCliCo
coastal climate core services

D5.1 State-of-the-art on coastal flood risk modelling of the European built environment

Release Status: FINAL

Dissemination level: Public

Author: Elco Koks (IVM-VU), Joël De Plaen (IVM-VU), Sadhana Nirandjan (IVM-VU), Jeremy Rohmer (BRGM), Rémi Thiéblemont (BRGM), Athanasios Vafeidis (CAU), Giovanna Pisacane (ENEA), Daniel Lincke (GCF)

Date: 24/02/2022

Filename and version: D5.1.docx

Project ID NUMBER 101003598

Call: H2020-LC-CLA-2020-2

DG/Agency: Name of Partner or Delivery representative

This project has received funding from the European Union's Horizon 2020 research and innovation programme under grant agreement No. 101003598

This project has received funding from the European Union's Horizon 2020 research and innovation programme under grant agreement No. 101003598

Document History

Location

This document is stored in the following location:

Filename	D5.1
Location	#WP5 in Teams

Revision History

This document has been through the following revisions:

Version No.	Revision Date	Filename/Location stored:	Brief Summary of Changes
V1	25/02/2022	#WP5	Initial

Authorisation

This document requires the following approvals:

Authorisation	Name	Signature	Date
Project Coordinator	Le Cozannet		25/02/22
WP Leader	Elco Koks	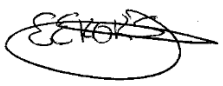	24/02/22

This project has received funding from the European Union's Horizon 2020 research and innovation programme under grant agreement No. 101003598

© European Union, 2021

No third-party textual or artistic material is included in the publication without the copyright holder's prior consent to further dissemination by other third parties.

Reproduction is authorised provided the source is acknowledged.

Disclaimer

The information and views set out in this report are those of the author(s) and do not necessarily reflect the official opinion of the European Union. Neither the European Union institutions and bodies nor any person acting on their behalf may be held responsible for the use which may be made of the information contained therein.

This project has received funding from the European Union's Horizon 2020 research and innovation programme under grant agreement No. 101003598

Executive summary

This report presents an overview of the current state-of-knowledge on exposure, vulnerability, risk and adaptation in relation to coastal flooding and the built environment. While the report has shown that there is a wealth of knowledge and data available at the start of this project, several gaps have been identified that need and will be addressed within CoCliCo. Firstly, improving the European coverage of geospatial data of critical infrastructure assets. While some infrastructure assets may have a good coverage of data availability across Europe through open-source initiatives such as OpenStreetMap (e.g., transport infrastructure), several infrastructures are also still far from complete (e.g., low-tier electricity networks). Secondly, we will make first steps in using social media and novel Natural Language Processing methods to develop a first set of vulnerability thresholds to provide a link between hazard intensity and network service functioning. This is currently mostly unknown within both a European and global context. Thirdly, development of future population exposure under different scenarios. This will provide the basis to identify how adaptation measures influence the development of population. Within CoCliCo, we hope to provide first answers. Finally, CoCliCo will make additional steps in developing a wide range of coastal adaptation measures for Europe, ranging from nature-based solutions to coastal migration. These measures will be incorporated within a risk modelling framework, allowing us to assess the potential benefits of each individual measure.

This project has received funding from the European Union's Horizon 2020 research and innovation programme under grant agreement No. 101003598

Table of Contents

This project has received funding from the European Union's Horizon 2020 research and innovation programme under grant agreement No. 101003598

This project has received funding from the European Union's Horizon 2020 research and innovation programme under grant agreement No. 101003598

1. Introduction

Critical infrastructure systems are the backbone of a prosperous society, playing an essential role in its day-to-day functioning (Hall et al. 2016; Hallegatte et al. 2019). They are, however, also exposed and vulnerable to natural hazards. As stated by Forzieri et al. (2018), port facilities and critical infrastructure networks in Europe are particularly vulnerable to coastal flooding and erosion. General climate change losses to critical infrastructure may increase tenfold by the year 2100, due to climate change alone (Forzieri et al., 2018). Critical infrastructure is important for the continuity of vital societal functions and is commonly associated with facilities such as the electricity grid, (tele)communication, transport, gas, water treatment plants and healthcare facilities. Protective infrastructures, such as levees, dams, and managed dunes and beaches, are essential to reduce the risk of flooding. Furthermore, it is important to highlight that the European Commission (EC) takes a much broader definition of infrastructure as is commonly used within the academic literature. More specifically, the EC includes all buildings (from private homes to schools or industrial facilities) and other physical assets (such as finance, food, government, research) within the concept of infrastructure (EC 2021/C 373/01). As such, this project will not only aim to assess the exposure and vulnerability of critical infrastructure as described in the academic literature, but will explicitly include all buildings, assets and networks within the built-environment as defined by the EC.

To avoid confusion around what we define by critical infrastructure within this project, we have decided to **not** entirely follow the definition by the EC, as this may cause confusion and unclarity in the remainder of this project. Within this project, we will refer to critical infrastructure when we indeed discuss critical infrastructure systems, such as the electricity grid, (tele)communication, transport, gas, water treatment plants and healthcare facilities. Other buildings within the built environment will be considered separately, and named what they are (e.g., residential buildings, industrial buildings.)

While the availability of geospatial information of infrastructure has improved tremendously over the last few years due to open-source initiatives (e.g., OpenStreetMap, OpenInfraMap, Corine Land Cover), several gaps still remain to make them useful for a comprehensive continent-wide risk analysis. Firstly, there is a coverage bias towards western Europe and high-density areas. Secondly, validation of open-source information is still lacking. As such, we often do not know whether the open-source information is mapped “correctly”. Thirdly, while the location of assets has seen a rapid increase in availability, the specific characteristics of these assets are often still unknown (e.g., voltage levels of a substation, capacity of a water treatment plant or hospital, building type). Finally, knowledge of network disruptions of infrastructure systems is still in its infancy, but essential in risk assessments.

Within the CoCliCo project, we aim to improve the risk assessment of infrastructure along the European coast. To do so, we will expand the geospatial information on exposure and vulnerability of infrastructure systems within Europe. This will include high-resolution mapping of infrastructure assets (i.e., exposure) and improve/create databases with the physical

This project has received funding from the European Union’s Horizon 2020 research and innovation programme under grant agreement No. 101003598

characteristics of these assets. Additionally, one should not forget the potential wider societal impacts as a result of infrastructure failures. As such, we will not only look at the physical elements within the coastal area, but also focus on the socioeconomic characteristics of the population living in Europe's coastal zone. This will mostly be done through the assessment of social vulnerability metrics. Finally, the risk framework will be enhanced through an explicit incorporation of a wide range of possible adaptation measures. This may range from nature-based solutions to migration away from the coastline.

This report will provide the starting point for the aforementioned proposed scientific advances. In Section 2, we will describe the concepts of exposure and vulnerability. In Section 3, we will provide an overview of the current state-of-the-art availability of exposure data. A similar overview is provided for vulnerability in Section 4. In Section 5, we introduce the proposed methods to fill in some of the existing knowledge gaps. Section 6 describes the risk assessment approach in CoClico, and in Section 7 we illustrate how we incorporate adaptation within CoCliCo's risk framework.

2. Definitions and concepts

We define risk as a function of hazard—the probability and severity of an event with potential to cause harm; exposure—the elements subject to the hazard; and vulnerability—the sensitivity of the element to hazards of given severity. The risk assessment in the CoCliCo project is performed in WP6, and the development of novel hazard maps is done in WP4. This leaves the developed of improved exposure and vulnerability knowledge for WP5.

2.1 Exposure

Within CoCliCo, we define exposure as all the elements that are potentially at risk to coastal flooding. This includes all assets, buildings, networks and people. Geospatial information of the elements that are exposed can be subdivided into two main categories: object-based (vectors) or grid-based (raster).

In grid-based approaches, the amount of infrastructure is typically determined using the (potential) percentage of infrastructural land use per grid cell in land cover maps such as CORINE (Coordination of Information on the Environment) or LUISA (Land Use-based Integrated Sustainability Assessment) (Büttner et al., 2014, Rosina et al., 2018). However, infrastructure, such as electricity lines and roads are typical narrow line elements and take up only a small percentage within a typical grid size for continental-scale modelling (e.g., 100×100 m2 in Europe). As these (assumed) percentages are often applied uniformly among the same land use type, this may result in an overestimation of infrastructure damage when there is in reality no infrastructure, but it may be an underestimation if the infrastructure is there but is not enough to be the dominant land use type (van Ginkel et al., 2021).

This project has received funding from the European Union's Horizon 2020 research and innovation programme under grant agreement No. 101003598

Object-based information show the exact outlines of each asset, building or network. This information provides a high-level of detail, and allows for a much more exact damage assessment, under several reasons. First, considering the geometric boundaries of an asset allows for more accurate intersects between the exposed roads and the hazard data. Object-based information generally has a higher resolution compared to grid-level information. Of course, this may be different on high-resolution local-scale assessments (e.g., when a 5x5m resolution is used), but this high-resolution grid-data is not readily available on continent-level. And if available, it is most likely a simple rasterization of object-data. Second, object-specific attributes (e.g., the width of the road, whether its paved or electrified) can be used to make more accurate damage estimates (Merz et al., 2010). For example, for an intersect between an electricity network and an inundation map, it is crucial to differentiate a high-voltage line with a low-voltage line, as they will result in very different damages and cascading impacts. The attributes enable the development of different damage curves for different infrastructure types (e.g., motorway or rural road), which may have very different characteristics (e.g., number of lanes, width, quality, and maintenance standards). Third, the network properties of roads, enabling graph representations, can be maintained in an object-based approach (Gil and Steinbach, 2008). This enables the study of direct infrastructural flood damage in coherence with other sources of impacts, such as travel delay times from road closures and detours, as well as indirect economic losses from passenger or freight delays (van Ginkel et al., 2021).

2.2 Vulnerability

Within CoCliCo, we distinguish between physical and social vulnerability. Physical vulnerability describes the susceptibility of assets or buildings to the flood. It generally describes how an asset or building will be damaged by a certain level of intensity of the flood. Social vulnerability, on the other hand, describes the characteristics of people in the flood-prone area and their potential vulnerability to a flood event. This section will further elaborate and describe the two different vulnerability types.

2.2.1 Physical vulnerability

Physical vulnerability is generally described through the relationship between the intensity of the hazard (e.g., flood depth or flow velocity) and the susceptibility of the respective asset or building. This relationship is most often referred to as vulnerability (absolute values) or fragility curves (relative values). In the case of flooding, these curves are often called depth-damage functions, which describe the relation between the land use/object type and the flood depth. To date, virtually all European-wide flood risk studies (Bouwer et al., 2018; Dottori et al., 2020; Lincke et al., 2019) still rely on the comprehensive set of damage curves proposed by Huizinga (2007) and Huizinga et al. (2017). See Section 4.1 for a more extensive description of Huizinga et al. (2017).

This project has received funding from the European Union's Horizon 2020 research and innovation programme under grant agreement No. 101003598

2.2.2 Social vulnerability

In the existing literature, several socio-demographic characteristics have been defined as determinants of social vulnerability. The most used characteristics are wealth, age and ethnicity (Cutter et al, 2003, Fekete, 2009). Several of these studies have applied a principal component analysis (PCA) to select the specific underlying variables from a wide range of options to be used for the vulnerability index.

2.3 Risk

Risk is formulated based on the European flood risk directive 2007/60/EC - consistent with IPCC definition (Weyer, 2021), as the "combination of the probability of a flood event and of the potential adverse consequences for human health, the environment, cultural heritage and economic activity (...)" (art. 2.2). In CoCliCo, we assess the consequences with respect to exposed people and damage to building environment by considering the interaction of the three components, namely coastal hazard, exposure, and vulnerability, hence providing a more complete vision on risk than popular extreme sea level metrics used in the climate and sea level community (see discussion by Rasmussen et al. 2020). Examples of global to regional scale coastal flood risk assessments for future climate conditions are provided by Vousdoukas et al. (2018) at European scale, by Hinkel et al. (2014) at global scale, and by Wing et al. (2022) for US (including the impact of rainfall, river flows or coastal water levels). Sect. 5 provides the procedure that is planned in CoCliCo for coastal flood risk calculation at European scale.

To describe the general stages for risk calculation procedure, we restrict here the presentation to the assessment of the projected expected annual damage (EAD) under relative sea level change (RSLC) (e.g., Aerts et al., 2013; Rasmussen et al., 2020). The calculation of other risk metrics follows similar steps. EAD is defined as:

$$EAD = \int_{x_{min}}^{\infty} \int_{\delta}^{\infty} d(x) f_{ESL}(x - \delta) f_{RSLC}\ (\delta) d\delta dx$$

where $f_{ESL}(.)$ is the probability density function of extreme sea levels (ESL) after considering RSLC δ (provided by WP3) whose probability density function is $f_{RSLC}(.)$,x_{min} is the height of the assumed current protection level (data provided by WP5), and d(.) is the cumulative damage function (provided by WP5 using coastal hazard intensity maps from WP4). When the latter is expressed in terms of monetary impacts, EAD is the expense that would occur in any given year if monetary damages from all hazard probabilities and magnitudes were spread out equally over time, i.e., the area under the risk curve as schematically depicted in Figure 1. Note that when RSLC is a defined based on a scenario (instead of a full probability distribution), the formulation corresponds to the one of DIVA model (with refined flooding algorithm version 2.4.1, see details in Hinkel et al., 2014).

This project has received funding from the European Union's Horizon 2020 research and innovation programme under grant agreement No. 101003598

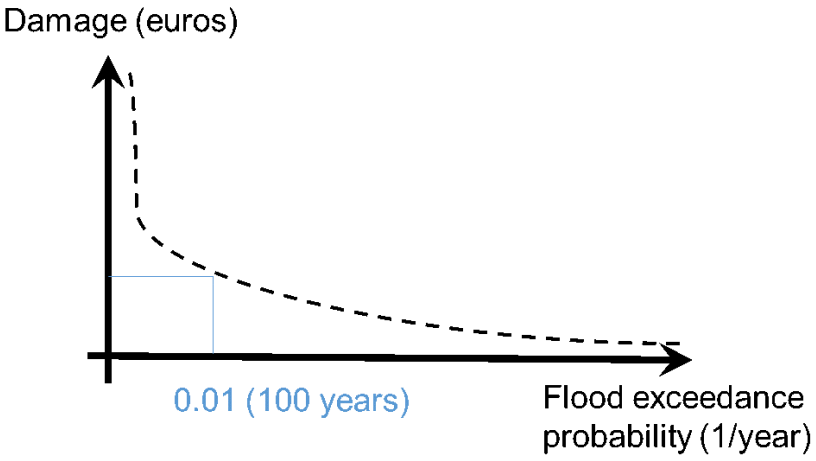

Figure 1. *Example of risk curve to compute EAD (as the area under the curve).*

In this case, the cumulative damage function is used to evaluate the damage costs to assets (e.g., residential buildings, critical infrastructures, etc. - data provided by WP5) induced by a flood of height *x* (provided by WP4) through the integration from elevation level 0 to *x* over the product of the vulnerability function *vul(.)* applied to the water depth *x−y* and of the derivative of the cumulative exposure function applied to the elevation level *y* as follows

$$d(x) = \int_0^x vul(x-y)e'(y)dy$$

The cumulative exposure function is computed based on WP4 analysis and gives the number of assets (using data provided by WP5) located below a given elevation level *x*. When considering population (using data provided by WP5), the calculation can be simplified by considering that damage function for population equals the cumulative exposure function, i.e., d(x)=e(x).

2.4 Adaptation

We understand adaptation as every measure that reduces risk. In terms of flood risk that can be specified as every measure that reduces flood risk. Our methodological approach towards adaptation consists in modelling the three generic responses to sea-level rise: protection, accommodation and retreat (SROCC, 2019). Under protection we understand any kind of measure that alters the flood hazard by preventing flood water to flow inlands, e.g., dykes or seawalls. These can be hard structures such as dikes and sea walls, but also nature-based solutions as beach and wetland nourishment. Other large-scale measures for flood protection exists (e.g., river barriers like the Thames barrier or closure dams like the proposed Northern European Enclosure Dam) but are behind the scope of CoCliCo. Accommodation describes every measure that alters the vulnerability layer by reducing damages at flooded assets, e.g., by flood proofing houses and infrastructure or elevating of assets. Retreat describes every

This project has received funding from the European Union's Horizon 2020 research and innovation programme under grant agreement No. 101003598

measure that adjusts the exposure layer by removing assets and population out of the coastal zone, such as displacement and managed realignment.

2.5 Critical Infrastructure systems

Within CoCliCo, we represent the critical infrastructure network by seven overarching Critical Infrastructure (CI) systems: *energy, transportation, telecommunication, water, waste, education,* and *health* (Hall et al. 2016; Nirandjan et al., in press). This is in line with the classification of infrastructure systems discussed in literature, whereby CI related to health and education have been receiving increasing attention. We use OpenStreetMap (OSM) as the baseline for most infrastructure data (see Section 3.2) within CoCliCo. And we will re-organize other infrastructure data, if possible, into OSM's typology structure. To extract relevant infrastructure types, we apply a combination of 97 active OSM tags to represent 42 infrastructure types that are categorized under the seven overarching CI systems. Table 1 provides an overview of the 41 infrastructure types and its categorization that are considered in this project.

***Table 1**. List of infrastructure types considered in this project, categorized under ten CI subsystems and seven overarching CI systems.*

System	Subsystem	Infrastructure type	System	Subsystem	Infrastructure type
Energy	Power	i. Cable ii. Line iii. Minor line iv. Plant v. Substation vi. Power tower vii. Power pole	Water	Water supply	viii. Water tower ix. Waster well x. Reservoir (covered) xi. Water works
Transportation	Railways	xii. Railway	Health	Healthcare	xiii. Clinic xiv. Doctors xv. Hospital xvi. Dentist xvii. Pharmacy xviii. Physiotherapist xix. Alternative xx. Laboratory xxi. Optometrist xxii. Rehabilitation xxiii. Blood donation xxiv. Birthing centre
	Roads	xxv. Motorway xxvi. Trunk xxvii. Primary xxviii. Secondary xxix. Tertiary xxx. Other			
	Airports	xxxi. Airport			
Telecommunication	Telecom	xxxii. Communication tower xxxiii. Mast			
Waste	Solid waste	xxxiv. Landfill xxxv. Waste transfer station	Education	Education	xxxvi. College xxxvii. Kindergarten xxxviii. Library xxxix. School xl. University

This project has received funding from the European Union's Horizon 2020 research and innovation programme under grant agreement No. 101003598

3. Overview exposure data

3.1 Building assets

3.1.1 OpenStreetMap

OSM has proven to be the most extensive dataset of publicly available building footprints for Europe. Full coverage for a certain region or country is primarily driven by the responsible public authority in a given region or country. If they decide to publish the building database publicly, it is only a matter of time before it will be included into OpenStreetMap. This happened, for instance, in the Netherlands and France. For countries where the building database is not publicly shared, such as the United Kingdom, the OSM database primarily depends on users who geo-reference buildings manually (Koks and Haer, 2021).

Koks and Haer (2021) compared the OSM building count with the reported building stock from the EU building database, to get a feeling on its completeness. The EU building database contains information on dwellings and non-residential buildings. Dwellings are places of residence such as a house, flat or an apartment. Their results show that countries like Austria, the Netherlands, France, Switzerland, and Poland have good coverage, while Spain, Portugal, and the United Kingdom experience a lower coverage. It is important to acknowledge the limitations of the incomplete database, which likely results in underestimation of damages. Overall, we consider the OSM dataset as a good starting point that provides building coverage in an open access dataset with coverage on an EU-wide level. Additionally, due to its almost real-time updates, the dataset will only further improve in the future.

3.1.2 National databases

Most countries within Europe have some form of centralized building registration system, of which some have their (geospatial) data publicly available. One example is the Basisregistratie Adressen en Gebouwen (BAG, Basic registration of Addresses and Buildings), which provides a full geospatial coverage of buildings, and their use and age, within the Netherlands. Similar datasets are available in other countries, either on national or subnational level. For example, Estonia has provided 3D footprints of all buildings within the country (Geoportal Estonia). For Italy, data about buildings are available as OGC services (WMS for visualisation and querying, WFS also for downloading), and are accessible via the National Geoportal[1]. Such data only cover the main urban areas of the country and contain the 3D geometry of each building polygon. In addition, the Italian Civil Protection Department has released the national dataset of structural aggregates, a highly detailed collection of data on the urban building footprints in Italy, mainly created from the information contained in the geo-topographic databases of the Italian Regions and Autonomous Provinces. The dataset is released under the Open CC-BY

[1] http://www.pcn.minambiente.it/mattm/en/

This project has received funding from the European Union's Horizon 2020 research and innovation programme under grant agreement No. 101003598

4.0 licence for the open use of all interested parties and available for free use, via the GitHub platform[2].

3.1.3 European data about building characteristics

A useful non-geospatial source of information to fill gaps within the data is the EU building database. This database contains information 250 different indicators on building characteristics within Europe. This ranges from building type and use, age, and engineering characteristics. While this information is only available on a country-level, it can help to further improve the baseline information from OpenStreetMap and/or national databases.

3.1.4 Other global sources

The PAGER database allows us to add additional exposure characteristics to the buildings, when unavailable for the respective country. This database gives information on the main construction types for buildings for each country. More specifically, the database provides information on the specific use of building types for (i) urban residential, (ii) urban non-residential, (iii) non-urban residential and (iv) non-urban non-residential. The database differentiates between 106 different building types. For example, this would mean that we assume that the building type of high-residential urban area in the Netherlands relates to the building types specified as urban residential for the Netherlands in the PAGER database.

3.2 Critical infrastructure assets

3.2.1. OpenStreetMap

As mentioned in Section 2.3, OSM will be used as the basis for the geospatial representation of infrastructure assets within the CoCliCo project, building upon previous successful work (e.g., Koks et al., 2019; Koks and Haer, 2021; Nirandjan et al., in press). The geospatial information on CI that we extract from the publicly available OSM dataset is stored in three different datatype formats: *point, line* and *polygon* (Figure 2). Firstly, a *point* feature represents a specific point in space and is defined by its latitude and longitude. Telecommunication towers, for example, are stored as *point* features in OSM. Secondly, a *line* feature is a segment that is connected by two or more point features. Linear infrastructures such as roads and cables are stored under the *line* datatype format. Lastly, a *polygon* feature is represented by a connection of line features, whereby the last point is connected to the beginning. Infrastructure types like hospitals, universities and airports are stored as polygons.

[2] https://github.com/pcm-dpc

This project has received funding from the European Union's Horizon 2020 research and innovation programme under grant agreement No. 101003598

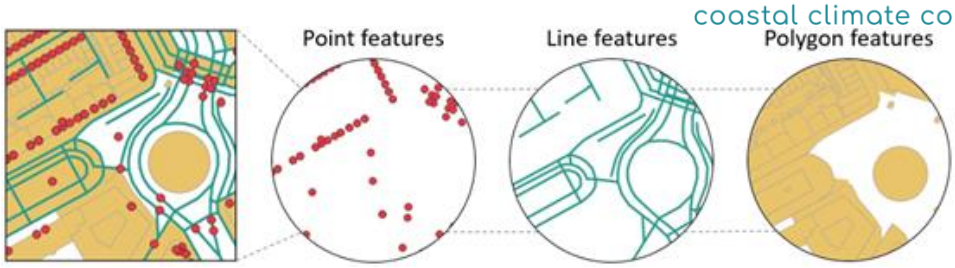

Figure 2. *Visualization of raw Open Street Map data of a given area, with a breakdown by the datatypes. Adapted from Nirandjan et al. (in press).*

3.2.2. National databases

In Italy, data about critical railways can be retrieved from the National Geoportal, by means of OGC services (WMS for visualisation and querying, WFS also for downloading). Concerning other infrastructures, data are not provided at the national level, but they are made available through local Geoportals/Repositories managed by the Regions[3]. Alternatively, the RNDT Catalogue[4] can be exploited to retrieve data about a specific infrastructure. The Catalogue provides information on the metadata for spatial data and services as documented by the competent administrations in Italy. Finally, the Italian National Institute of Statistics provides an Atlas of National Infrastructures (ASTI - http://asti.istat.it/), that is useful for statistical purposes.

3.2.3 European specific databases (e.g., T-NET)

ENTSO-E[5]

The database provides information on transmission lines operated by members of the European Network of Transmission System, Mediterranean Transmission System Operators, System Operator of the UPS of Russia and UKRENERGO National Power Company. The database includes lines of 220kV and higher. Although a map is available, the assets are not precisely georeferenced. Thus, the database gives rather an approximative indication of the location. The database also includes parts of Northern Africa and parts of Russia.

The European Pollutant Release and Transfer Register (E-PRTR)[6]

The database contains annual data of over 30.000 industrial facilities covering 65 economic activities within nine industrial sectors (energy, production and processing of metals, mineral industry, chemical industry, waste and wastewater management, paper and wood production

[3] https://www.cisis.it/?page_id=3185

[4] https://geodati.gov.it/geoportale/eng/

[5] https://www.entsoe.eu/data/map/

[6] https://prtr.eea.europa.eu/

This project has received funding from the European Union's Horizon 2020 research and innovation programme under grant agreement No. 101003598

and processing, intensive livestock production and aquaculture, animal and vegetable products from the food and beverage sector, and other activities).

3.2.4. Other global databases

Several global databases complement OpenStreetMap with additional georeferenced information on infrastructure assets.

Predictive mapping of the global power system with Gridfinder[7]
The global power network dataset consists of a composite map created using the open-source tool *gridfinder.* The dataset, based on the work by Rohr at Facebook, provides a connected network at two voltage levels: a high voltage level (>70kV), and a medium voltage level (10-70kV). To create the map, the gridfinder tool applies filtering algorithms to night-time imagery to identify locations that are the most likely to produce light from electricity. Those light-producing locations are then connected to known electricity networks following roads and known distribution lines from OpenStreetMap (Arderne et al., 2020).

Global Database of Power Plants[8]
The database provides 30.000 georeferenced power plants from 164 countries. Each entry also includes information on the capacity, generation, ownership, and fuel type of the plant. The power plants referenced consist of both thermal (e.g., coal, gas, oil, nuclear, biomass, waste, geothermal) and renewable energy (e.g., hydro, wind, solar). The collection process was achieved using reliable and publicly available sources on a country-to-country basis. This includes data from national government agencies, reports from constructing and components providing companies, data from public utilities, and information from multinational organizations (Bryers et al., 2020).

ENERGYDATA.INFO[9]
The database is an initiative from the World Bank Group. It provides an open data platform to access submitted datasets and data analytics that are relevant to the energy sector. This includes submissions from the World Bank Group, Bloomberg New Energy Finance, Building and Urban Data Science Lab, Columbia University Earth Institute, Duke University Energy Initiative, Facebook and more. The country-based datasets contain information on substations, electrical transmission networks, renewable power plants but also wind measurement and irradiance data.

Carbon Monitoring for Action (CARMA)[10]
CARMA is a global database initially aimed at monitoring carbon emissions. It also gathers georeferenced information on 50.000 power plants and the 4.000 firms owning them until 2012.

[7] https://zenodo.org/record/3538890

[8] https://datasets.wri.org/dataset/globalpowerplantdatabase

[9] https://energydata.info/dataset

[10] http://carma.org/

This project has received funding from the European Union's Horizon 2020 research and innovation programme under grant agreement No. 101003598

Power Reactor Information System (PRIS)[11]
PRIS focuses on nuclear power plants worldwide. It contains information on power reactors in operation, under construction, or those being decommissioned. It also includes reactors information such as status, location, operator, owner and supplied. The database is maintained by the International Atomic Energy Agency (IAEA).

Think Geo Energy[12]
The dataset provides georeferenced data on geothermal and hydrothermal plants. It is maintained by a service company delivering business-to-business news on the sector.

OpenCelliD[13]
The dataset contains georeferenced cell towers. The database relies on uploads from the community. As of now, it includes almost 36 million unique towers.

New Cloud Atlas[14]
The database is part of an effort to provide a georeferenced open platform for the physical locations making up the cloud. This includes warehouse data centre, internet exchange, each connecting cable and switch. The database uses OpenStreetMap to ensure its accessibility and to facilitate contributions.

OpenInfraMap[15]
The project captures the world's infrastructures georeferenced within OpenStreetMap that are not shown by default. This includes power plant and transmission, solar generation, oil and gas, water, and Telecommunication.

Planet[16]
Planet provides automatically generated maps of buildings and roads. The private company is specialised in providing geospatial analysis services. The maps created for a handful of countries has been achieved using, satellite imagery, deep learning and cloud computing.

OpenSeaMap[17]
OpenSeaMap is an open-source project aimed at providing a free nautical database for sailors. The database also includes georeferenced harbours and ship supply information from OpenStreetMap and MarineTraffic.

[11] https://pris.iaea.org/pris/

[12] http://www.thinkgeoenergy.com/map/

[13] http://wiki.opencellid.org/wiki/What_is_OpenCellID

[14] http://newcloudatlas.org/about.htm

[15] https://openinframap.org

[16] https://www.planet.com/pulse/mapping-all-of-earths-roads-and-buildings-from-space/

[17] http://map.openseamap.org/

This project has received funding from the European Union's Horizon 2020 research and innovation programme under grant agreement No. 101003598

Healthsites.io[18]
Healthsites.io provides an open platform for georeferenced database of health facilities globally such as hospitals, doctors, pharmacies, and dentists. The database is updated through users, partners and OpenStreetMap.

The GlObal geOreferenced Database of Dams (GOOD)[19]
The database contains more than 38.000 dams and their associated catchment. It is produced through digitisation of satellite imagery, and thus, includes large to medium concrete dams that are observable from LANDSAT, IKONOS and SPOT imagery (Mulligan et al., 2020).

World Food Program Global Ports[20]
The database contains harbours' locations. The data are gathered by the WFP logistics cluster. Additional information also includes the size of the harbour, maximum depth, and length of the vessels.

Openflights Airports Database[21]
The database contains 9.300 georeferenced airports around the world. The data are DAFIF and OurAirports.

3.3 Population data

In recent years, several global spatial population datasets have been developed and used in broad-scale flood exposure and risk assessments (Hinkel et al., 2014; Merkens et al., 2018; Vousdoukas et al., 2018; Tiggeloven et al., 2020, Kulp and Strauss, 2020). Table 2 presents the most commonly employed datasets in such global- or continental-scale analyses. These datasets use national population and census data as a basis for representing the spatial distribution of population and are provided in gridded format, at various resolutions. Due to errors inherent in the nature of census data (data gaps, date of acquisition, misallocation of people) the development of available global datasets has been based on different methods for addressing those errors and representing the spatial distribution of people as correctly as possible. Leyk et al. (2019) provides a list of the different factors that contribute to uncertainties in the final population data products.

The datasets in Table 2 have been further used as the basis for the development of scenarios of future population distribution. Before the emergence of the new scenario framework for climate impact research (i.e., the Representative Concentration Pathways (RCP) and the Shared Socioeconomic Pathways (SSP); O'Neil et al., 2014) most impact and vulnerability assessment studies would employ scenario-specific national scale population growth rates and assume a uniform population growth (e.g., Hinkel et al., 2014). Recent studies have

[18] https://healthsites.io/map

[19] http://globaldamwatch.org/goodd/

[20] https://geonode.wfp.org/layers/geonode:wld_trs_ports_wfp

[21] https://openflights.org/data.html

This project has received funding from the European Union's Horizon 2020 research and innovation programme under grant agreement No. 101003598

developed scenarios of the future spatial distribution of population by extending the scenario narratives and/or quantifying spatial differences in population growth based on the elements of the narratives. The most used global population projections are those of Jones and O'Neill (2016) who accounted for urban attraction and those of Merkens et al. (2016) and Reimann et al. (2018) who considered coastal attraction. Merkens et al. (2018) found differences of up to 72% in assessing future (2100) population exposure depending on the scenario and base dataset used.

***Table 2**. List of population global data (from Wolff, 2020)*

Population dataset	Reference year	Horizontal resolution	Disaggregation approach	Selected studies using the population data
GRUMP	1900, 1995, 2000	~1 km	Dasymetric (lightly modelled)	Merkens et al. 2016, Neumann et al. 2015, Hinkel et al. 2014, McGranahan et al. 2007, Lichter et al. 2011,
LandScan	1998, 2000 - 2017	~1 km	Smart interpolation (highly modelled)	Kulp and Strauss 2019, Lichter et al. 2011, Hinkel et al. 2014
GWP V3 V4	 1990, 1995, 2000, 2005*, 2010*, 2015* 2000, 2005, 2010, 2015*, 2020*	~5 km	Areal weighting (unmodeled)	Paprotny et al. 2018, Reimann et al. 2018, Jones and O'Neill 2016
GHS-POP	1975, 1990, 2000, 2015	250 m & 1 km	Dasymetric refinement, proportional to built-up density** (lightly modelled)	Vousdoukas et al. 2018
WorldPop	2000-2020	100m & 1km	Statistical (random forest) /dasymetric	Mainly used in national assessments to date, e.g., Yang et al. 2019, Ramirez et al. 2016

This project has received funding from the European Union's Horizon 2020 research and innovation programme under grant agreement No. 101003598

4. Overview of vulnerability information

4.1 Building asset vulnerability

As described in section 2, asset vulnerability is generally assessed using vulnerability or fragility curves, either on an object-level or grid-based. This section will provide an overview of some of the most used sources to assess damages to buildings, within Europe.

A comprehensive set of depth–damage curves (both continental and country scales, considering all continents and >200 countries) has been proposed by and Huizinga (2007) and Huizinga et al. (2017), which have been applied in many studies (e.g., Albano et al., 2017; Amadio et al., 2016, 2019; Carisi et al., 2018; Dottori et al., 2018b; Jongman et al., 2012; Prahl et al., 2018). In Huizinga et al. (2017), they differentiate between residential, commercial, industrial and agricultural use for building-specific land use types.

Depending on the metrics used to support decision making for coastal risk management, computing the impacts of storm surges and sea-level rise in coastal cities typically need also to go beyond physical damage assessments and to reflect the economic losses as well (like the expected annual flood cost, see e.g., Hinkel et al., 2014 for an example of marine flooding at global scale using Dynamic Interactive Vulnerability Assessment modelling framework). This economic assessment requires high-level information on the damage costs associated with varying flood heights. This can either be done by relying on a two-stage approach: (1) damage assessment (using depth-damage curves); (2) translation of damages into economic losses following the approach of Hinkel et al., 2014 and Hallegate et al.,2013. For this purpose, the global JRC model provides maximum loss values per continent and country (harmonized to the 2010 price level and to Euro) that can be used in combination to the depth-damage curves. More recently, Prahl et al. (2018) adapted the JRC country-scale damage-depth curves to provide a publicly available dataset (PANGEO data repository) for such depth - damage cost curves (with adjusted monetary estimates to 2016 price levels) for 600 European coastal city clusters (derived from CORINE 2012 data) at flood heights between 0.0 m and 12.0 m (based on the EVRS2000 vertical datum). They also provided data for protection costs as well. See some examples in Figure 3.

This project has received funding from the European Union's Horizon 2020 research and innovation programme under grant agreement No. 101003598

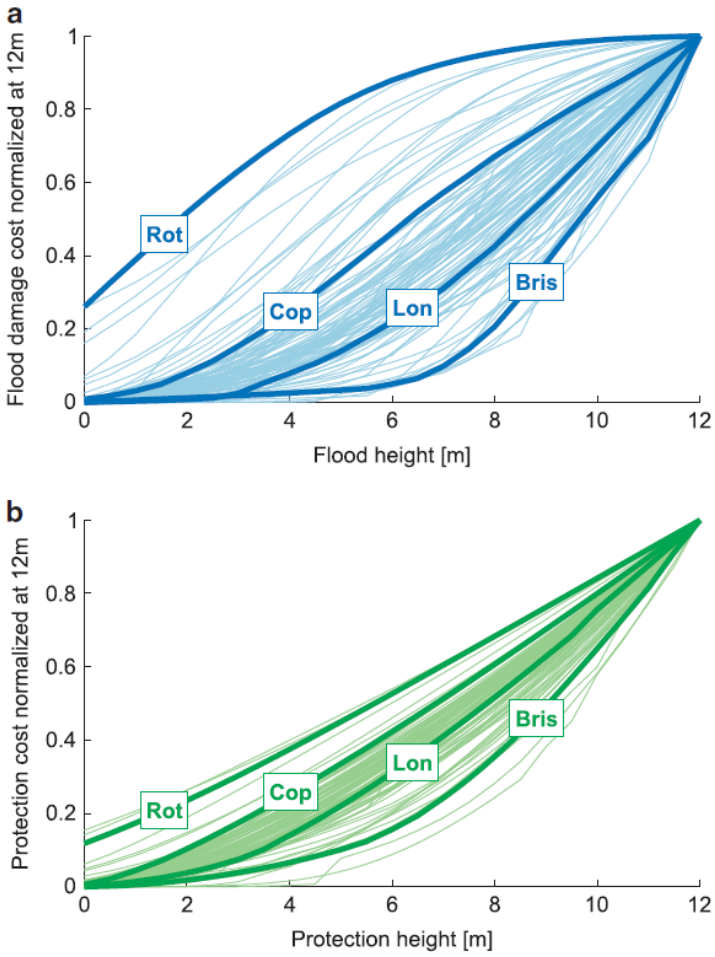

Figure 3. *Damage and protection cost curves for top 100 urban clusters with the largest area extracted from Prahl et al. (2018). (a) Normalized damage curves, where each curve has been divided by the damage at a hypothetical 12 m flood height. (b) Normalized protection cost curves, where each curve has been divided by the protection cost at the 12 m height. The curves for the cities of Rotterdam (Rot), Copenhagen (Cop), London (Lon), and Bristol (Bris) have been highlighted.*

A rich complementary source of information may be provided by the insurance sector. For instance, US Federal Emergency Management Agency released a dataset of >2 million from the National Flood Insurance Program. Yet, insurance data can be difficult to analyse and may be subject to large uncertainties (e.g., Wing et al., 2020; Andre et al., 2013; Diaz Loaiza et al., 2022). Feasibility to include them as inputs for CoCliCo activities at an operational level deserve further examination.

This project has received funding from the European Union's Horizon 2020 research and innovation programme under grant agreement No. 101003598

4.2 Critical infrastructure vulnerability

The vulnerability overview provided here builds upon the work of Nirandjan et al., (in progress).

4.2.1 Energy

Power plants

FEMA (2013) developed vulnerability curves for power plants with varying capacities. They categorize small, medium and large power plants, which are characterized by a power generation of <100 MW, 100-500 MW, and >500 MW (FEMA, 2021). A qualitative measure is given to the vulnerability of power plants to three measures of flood severity. Namely, power plants are highly vulnerable to inundation, but are not vulnerable to scour/erosion, and debris impact/hydraulic pressure. Hence, the vulnerability curve is in form of the relative damage as function of the inundation level. For the development of the damage functions, the depth of flooding within a power plant is compared to the height of critical components within the given power plant. Here, the general assumption is that electrical switch gear is located at a height of 0.91 m above ground level. Specifically for small power plants, they also assume that support facilities are damaged on ground level, and that control and generation facilities are damaged when flood water depths are reaching higher levels. Strikingly, the curve for the damage functions for the three categories of power plants are similar. For risk assessments, however, the vulnerability functions are used in combination with replacement costs, which vary depending on the capacity of the power plant.

Whereas FEMA (2013) provides vulnerability curves for power plants in general, the following technical background report indicates that the vulnerability of power plant types differs. Miyamoto International (2019) differentiates between thermal plants, hydro power plants, solar farms, wind farms and nuclear power plants. They assume that the vulnerability of thermal plants is similar to the aforementioned vulnerability curves developed by FEMA (2013). The vulnerability of hydropower plants, however, cannot be explained by such a depth-damage curve. One of the main functionalities of a hydropower plant is flood protection (e.g., the Three Gorges Dam in China), and therefore these structures may be subject to overtopping during a flood event. For solar farms, the vulnerability is predominantly associated with scour of the support frame of a solar panel, which could happen during an event of intense flash flooding. Furthermore, wind farms are not vulnerable to flooding, whereas nuclear power plants (NPPs) are. Bensi et al. (2015) point out that the evaluation of the susceptibility of the various components of NPPs as a function of the severity of a hazard, in combination with observations to reduce uncertainties, is an important next step to improve understanding about the flood fragility of NPPs. Kim et al. (2021) presents a methodology to develop tailored fragility curves for NNPs based on empirical data gathered by plant experts during an evaluation of fragile structures (e.g., flood proof doors) and facilities (e.g., cooling water building), design data of the NNPs, satellite data, and by determining threshold heights of (connected) facilities to evaluate potential flood pathways in case of internal flooding using a probabilistic approach. Specifically, for the NNPs under consideration was determined that if the water depth reaches a critical level, the flood water starts entering facilities at ground level,

This project has received funding from the European Union's Horizon 2020 research and innovation programme under grant agreement No. 101003598

and then propagates down through the stairs into the motor control centre (MCC). The developed fragility curve for the MCC is a lognormal distribution, depicting the probability of damage (causing a failure) as a function of the water depth. This function can be applied for probabilistic flood analysis as presented by Kim et al. (2021).

Substations

Fragility curves are developed for substations with varying capacities (FEMA, 2013). Here, substations with the functionality transmission (138-765 kV) and sub-transmission (34.5-161 kV) are considered, which are further categorized as small (low voltage: 34.5-150 kV), medium (medium voltage: 150-350 kV), and large (high voltage: >350 kV) substations. Similar to the fragility curves developed for power plants, the vulnerability curve is in form of the relative damage as function of the inundation level as substations are highly vulnerable to inundation and not to scour/erosion, and debris impact/hydraulic pressure. Here, the general assumption is that electrical switch gear is located at a height of 0.91 m above ground level, damage to the control room starts at the onset of the flood and is maximized when reaching a water level of 2.13 m, and that electrical components (e.g., cabling, transformers, and switchgear) are damaged as well. Strikingly, the curve for the damage functions for the three categories of substations are similar. For risk assessments, however, the vulnerability functions are used in combination with replacement costs, which vary depending on the capacity of the power plant.

Transmission and distribution systems

FEMA (2013) developed three fragility curves for the distribution circuit, which we distributed amongst the infrastructure type cable (i.e., underground T&D system) and power (minor) lines (i.e., overhead T&D system). Underground and aboveground infrastructure is assumed to stay unharmed due to inundation, while there is a low vulnerability expected at the end of buried cables. Repair costs for distribution circuits are provided, but is lacking unit data and thus making it unclear how to use these repair costs for risk assessments. We find observational data that support the assumptions taken for the development of these fragility curves. A survey was conducted on the underground transmission circuit performance during flooding due to major weather events among affected power utilities in the USA (Burns & McDonnel, n.d.). From this survey is concluded that underground assets are unlikely to suffer direct damage due to flooding. However, flooding is likely to impact the above grade equipment that the cables are connected with, and this failure may subsequently propagate into the whole energy circuit. However, uprooting of trees (Hall, 2009) and soil liquefaction (Miyamoto International, 2019) may cause damages to underground infrastructure.

4.2.2 Transportation

Roads

For use in raster-based models, Huizinga (2007) developed a set of damage functions for diverse land use classes including transport infrastructure, initially for the European Union (EU) and later generalized worldwide (Huizinga et al., 2017). Somewhat confusingly, these curves differentiate between the land use classes ‘transport’ and ‘infrastructure’. ‘Transport’ is defined as ‘transport facilities’ which seems to refer to transport terminals such railway

This project has received funding from the European Union’s Horizon 2020 research and innovation programme under grant agreement No. 101003598

stations, and ports. 'Infrastructure' is defined as physical damage to "roads and railroads as a result of contact with (fast flowing) water" (Huizinga et al., 2017, p.96). Although the curve is wider applied to diverse infrastructure classes, the background document (Huizinga, 2007) shows that it is explicitly derived for road infrastructure. Moreover, it shows a great variety in the input data from which the final curve was constructed; with a max damage value ranging from 0 to 65 €/m^2 that is reached at a water level ranging from 0.5 to 6 m, and a spectrum from smooth incremental curves to curves with one single jump from 0 to 100% of maximum damage. This variety shows that the final smooth exponential curve towards 24 €/m^2 at 6 m water depth hides large variability. An empirical verification by Jongman et al. (2012) confirms this variability, showing that curves well predict damage for one case in Carlisle, but are very far off for another case in Eilenburg.

For use in asset-based models, van Ginkel et al. (2021) developed a new set of damage functions specifically for roads in the EU and compare these to the Huizinga (2007) infrastructure function. In the absence of validation data, the new curves draw on an inventory of road construction and repair costs. The first differentiation in the curves is that the max damage costs are tailored to six different road types in OpenStreetMap (OSM) while correcting for the number of lanes. A second differentiation in the shape of the curve assumes that motorways and trunk roads are located on 1-m high embankments and the other roads on surface level. For motorways and trunks, a third differentiation is made between 'sophisticated' vs. 'simple' designs, referring to the presence of expensive and vulnerable road accessories such as electronic signalling. A fourth differentiation for all road types is between an upper and lower limit of flow velocities that can reasonably be expected for large-scale river flooding; aiming at use in depth-damage flood models while at the same time acknowledging that flow velocity is at least as important as water depth (Koks et al., 2021; Kreibich et al., 2009). Surprisingly, Van Ginkel et al. (2021) find that an object-translation of the Huizinga (2007) curves result in only slightly lower values, well within the 50% uncertainty interval of the new curves. However, Van Ginkel et al. (2021) also show that with the new curves, much more damage is attributed to motorways and trunks, and much less damage to the other road types. An important limitation of the Van Ginkel et al. (2021) curves are that damage to bridges is completely ignored, whereas empirical research suggests that this can be a major source of damage (Jongman et al., 2012; Koks et al., 2021).

Railways

A damage function for railways is developed by Kellermann et al. (2015) using the RAilway Infrastructure Loss (RAIL) model that estimates the direct damages to railway infrastructure derived from empirical flood damage data. They use the March River flooding of 2006 as a case study, whereby photographic documentation of flood damage to a double-tracked Austrian Northern Railway line is used to identify three stages of damage. The railways are assumed to be a standard double-tracked railway cross-section that consists of the following elements: substructure, superstructure, catenary and signals. The first damage class relates to the substructure of the railway that is (partly) impounded by water, but results in only little damage. The second damage class assumes that the substructure and superstructure of a

This project has received funding from the European Union's Horizon 2020 research and innovation programme under grant agreement No. 101003598

track segment is completely flooded, which is expected to result in damage to at least the substructure. The final class assumes damage to the superstructure, catenary and/or signals, and that complete restoration is needed for the standard cross-section of the affected track segment. The damage states are linked to damage estimates by correlating hydraulic impacts and damage stages, identifying impact parameters and determining associated thresholds.

A railway damage function and an associated cost feature is presented by Kok et al. (2005) for double-tracked railways in low-frequency flood areas. The damage function has a slowly increasing slope, reaching a damage of 100% only at an inundation level of 5 m. National data on railway damages is used for the development of the maximum damage (Briene et al., 2002). Furthermore, for application in high-frequency flood areas, the maximum damage can be lowered by 25% as a lower damage is expected in these areas due to risk-reducing measures (Kok et al., 2005). The railway system consists of facilities such as bridges, tunnels, stations and maintenance facilities. Damage functions for these railway facilities and tracks as well as for light railway systems will be developed as part of the new technical report on the HAZUS flood model (FEMA, 2013).

Airports

A damage function, showing the relation between the relative damage and the inundation depth, and the associated costs for airports in low-frequency flooded areas is presented by Kok et al. (2005). The damage function shows that 50% of the damages occur with an inundation level of 0.5 m, and is maximized when the floodwater reaches a depth of 3.6 m. The curve, however, is also used for land-use with the occupation agriculture and recreation. The maximum damage is based on two components: the direct damage based on construction costs per ha, and the direct damage based on the replacement value for airplanes (Briene et al., 2002). The total maximum damage is estimated to be 1,197EU/m^2, with the construction and replacement costs being 650EU/m^2 and 547EU/m^2, respectively. Furthermore, the similar damage function may be extended to high-frequency flooded areas, but with lower maximum damages as is expected that risk-reducing measures are implemented during the construction phase of airports in these areas (Kok et al., 2005). Airports, however, are systems that are composed of multiple elements: (un)paved runways, control towers, terminal buildings, aprons, fuel facilities, and maintenance and hanger facilities. The evaluation of the relation between flood intensity and damage to facilities of airports is expected to be published with the release of a new technical report on the HAZUS flood model (FEMA, 2013).

4.2.3 Telecommunication

Kok et al. (2005) provides a damage function and an associated maximum damage amount for the estimation of flood risk to communication systems in diked areas in the Netherlands. The flood damage is determined by flood depth, and the damage function is given as the damage factor as a function of the water depth. The damage function, however, is not specifically developed for elements within the communication system. In combination with the maximum damage, the data can be applied to calculate the physical damage per building that provides communication services. The maximum damage is based on depreciation costs over

This project has received funding from the European Union's Horizon 2020 research and innovation programme under grant agreement No. 101003598

a period of five years as an approximation for the replacement value (Briene et al., 2002). Furthermore, the vulnerability data allows for application to high-frequency flooded areas (i.e., return period of higher than 25 years) by adjusting the maximum damage. For the Netherlands, the assumption is that flood risk is accounted for during construction, and the maximum damage thus can be reduced by 25% for risk assessments in high-frequency flood areas.

FEMA (2013) formulated a classification for the telecommunication system. This classification includes communication lines, and a range of telecom facilities. Even though repair costs are determined for communication lines and replacement costs for various facilities, fragility curves for these elements will be developed as part of a new technical report on flood risk assessments. However, a qualitative measure of the vulnerability of power plants to three measures of flood severity is provided. Switching stations and access vaults are highly vulnerable to inundation, while buried transmission/distribution lines at river crossings are highly vulnerable to scour and erosion processes. A low to medium vulnerability due to debris impact/hydraulic pressure processes is assigned to telecom infrastructure.

4.2.4 Water

FEMA (2013) provides vulnerability curves and reconstruction costs for (potable) water system facilities, including water treatment plants, pumping stations, storage tanks and wells. Large reservoirs, which can be both natural) artificial, are usually created by using a dam, and are part of this (potable) water system. Dams are subject to overtopping during extreme flooding, and this could be prevented by drenching to remove excess sediment, a smart spillway design (e.g., adequate capacity and remote operation), and increase the freeboard (Miyamoto International, 2019).

Water treatment plants

A range of damage functions are developed by FEMA (2013) for water treatment plants (WTP), that are generally composed of a number of interconnected pipes, basins and channels required for physical and chemical processes to improve water quality. WTPs with a capacity of 38-189 million L/day are categorized as small WTPs, WTPs with a capacity of 189-757 million L/day are categorized as medium WTPs, and WTPs with a capacity above 757 million L/day are categorized as large WTPs (FEMA, 2013). In addition, the building design is taken into account as well, hereby differentiating between designs that are open and closed, and whether they are pressurized. In general, the damage functions for open WTPs follow the same curve, and the ones developed for closed and pressurized WTPs as well. Here, the damage functions developed for open WTPs assume a higher vulnerability compared to the closed and pressurized WTPs. Moreover, additional curves are developed for open WTPs, and closed and pressurized WTPs that represent less than average damage and more than average damage.

Storage tanks

A total of five damage functions were developed by FEMA (2013) for storage tanks, that typically have a capacity of 1.9- 7.6 million L/day (FEMA, 2021), with varying elevation levels

This project has received funding from the European Union's Horizon 2020 research and innovation programme under grant agreement No. 101003598

(i.e., at grade, elevated, or below grade), and construction materials (i.e., wood, steel, or concrete). The damage functions developed for storage tanks at grade level and elevated storage tanks are not vulnerable to inundation levels. For the first category of storage tanks is assumed that the water level in the tank, that is at grade level, exceeds the flood depth, thus preventing the storage tank from floating. For the second category of storage tanks is assumed that the tank foundations are not damaged. However, storage tanks that are situated below grade are assumed to be vulnerable to flooding, with the underlying assumption that the tank vent is 0.91 m above grade, and that cleanup will be required after flooding.

Water well

FEMA (2021b) refers to water wells that typically have a capacity between 3.8 and 18.9 million L/day. A damage function is developed assumes that electrical equipment and well openings are 0.91 m above ground level, and that a well is not permanently contaminated after flooding.

Pumping plant

Pumping plants are typically composed of a building, one or more pumps, electrical equipment and occasionally with backup power systems. FEMA (2013) developed damage functions for pumping plants on basis of elevation level and capacity. Small pumping plants have a capacity of lower than 38 million L/day, medium pumping plants have a capacity 38-189 million L/day, and large pumping plants have a capacity of more than 189 million L/day. The vulnerability of a pumping plant, however, is determined by the elevation level. For pumping plants below grade is assumed that the entrance is 0.91 m above grade. Flood water starts entering the pumping plant once this critical height is exceeded, hereby damaging electrical equipment that is assumed to be below grade. In contrast, the damage function for pumping stations above grade propagates gradually.

Kok et al. (2005) presents a damage function for pumping stations which can be used in combination with a cost value to estimate the direct physical damage to pumping stations in diked areas in the Netherlands. The inundation level of the flood water is used as the intensity measure in the damage function, with a damage factor ranging between 0 to 1. The cost value is derived from the average of insured values of pumping stations located in the former water authority ‘Groot Haarlemmermeer’ (Briene et al., 2002). Furthermore, the damage function is developed for pumping stations located in areas with a return period lower than 25 years with a capacity of 518 L/d.

Control vaults and stations

FEMA (2013) provides a damage function and associated reconstruction costs for control vaults and stations. They assume that the entrance is at grade and that water can enter control vaults and stations, resulting in a damage of 40% of the reconstruction costs.

Transmission pipelines

According to FEMA (2013), transmission pipelines for potable water are not expected to be harmed due to inundation levels, resulting in damage functions that represent a damage factor of zero for inundation levels for various categories of transmission pipelines. However, FEMA (2013) ranked a medium vulnerability level to debris impact/hydraulic pressure for pipelines at

This project has received funding from the European Union’s Horizon 2020 research and innovation programme under grant agreement No. 101003598

bridge crossings, and a high vulnerability to scour and/or erosion processes for pipelines situated at buried river crossings. Miyamoto International (2019) highlights that if water pipelines are empty, they may experience displacements as a result of buoyancy effects.

4.2.5 Waste

FEMA (2013) provides vulnerability curves components of the waste system, including associated reconstruction costs for waste system facilities and repair costs for pipelines.

Wastewater treatment plants

Iinfrastructure components of Wastewater treatment plants (WWTPs) are similar to the ones described for WTPs, but with the addition of secondary treatment subcomponents. Three damage functions were developed by FEMA (2013) for three categories of WWTPs according to capacity: lower than 189 million L/d (i.e., small WWTP), 189-757 million L/d (i.e., medium WWTP), and more than 757 million L/d (i.e., large WWTP). However, the form of the damage function is similar for the three categories of WWTPs, whereby it is assumed that cleanup, repair of small motors, buried conduits and transformers is required from the onset of the flooding. Cleanup and major repair of electrical equipment is required when the flood inundation level exceeds 0.91 m. In addition to these damage functions, damage functions are developed for WWTPs that have a higher and lower vulnerability.

Kok et al. (2005) presents a damage function for WWTPs which can be used in combination with a cost value to estimate the direct physical damage to WWTPs in diked areas in the Netherlands. The inundation level of the flood water is used as the intensity measure in the damage function, with a damage factor ranging between 0 to 1. The cost value is derived from the average of insured values WWTPs managed by a local water authority (Briene et al., 2002). Furthermore, the damage function is developed for WWTPs located in areas with a return period lower than 25 years.

Lift stations

A total of four damage functions were developed by FEMA (2013) for lift stations, which are facilities to pressurize the waste system aiming to raise sewage over topographical rises. If such a lift station is disrupted, untreated sewage may spill out near the lift station, or flow back into a collection sewer system (FEMA, 2021). Lift stations are classified as either small (capacity less than 38 million L/d), medium (capacity between 38-189 million L/d), or large (capacity more than 189 L/d), and whether the lift station is flood proof. The non-flood proof lift stations are assumed to be damaged by flood water up to 40% of the reconstruction costs, while flood-proof lift stations may experience a damage only up to 10%.

Control vaults and stations

FEMA (2013) provides a damage function and associated reconstruction costs for control vaults and stations. They assume that the entrance is at grade and that water can enter control vaults and stations, resulting in a damage of 40% of the reconstruction costs.

This project has received funding from the European Union's Horizon 2020 research and innovation programme under grant agreement No. 101003598

Sewers & interceptors

FEMA (2013) defines three categories for the waste transmission system, assuming that no damage is expected from submergence. However, FEMA (2013) ranked a medium vulnerability level to debris impact/hydraulic pressure for pipelines at bridge crossings, and a high vulnerability to scour and/or erosion processes for pipelines situated at buried river crossings. Miyamoto International (2019) highlights that if sewer pipelines are empty, they may experience displacements as a result of buoyancy effects.

4.2.6 Health & Education

Huizinga et al. (2017) developed vulnerability data for the category 'commercial buildings', which also includes schools and hospitals. A depth-damage function is generated for Europe, North America, Central- and South America, Asia, Oceania, and at the global scale based on flood damage data and country-specific quantitative. Maximum damages are computed for all countries using regression techniques, and also a world average is presented. In addition to this, maximum damage is provided for building-based risk assessments, land-use based, and object-based.

Kok et al. (2005) present a general depth-damage function that can be applied for companies in low-frequency flooded areas. Education institutions (e.g., universities) and social services (e.g., hospitals) are categorized under the 'government' damage category. The maximum damage is computed based on depreciation costs over a certain timeframe in years as an approximation for the replacement value (Briene et al., 2002).

FEMA (2013) provides damage functions for essential facilities, which includes both health facilities and education facilities. More specifically, damage functions are available for hospitals (with varying capacities), medical clinics (e.g., clinics, labs, and blood banks), schools (i.e., primary/secondary schools), and colleges/universities (i.e., Community and State colleges, State and Private Universities). These damage functions, however, are only accessible via the HAZUS software, and are thus not included in our database. The damage to essential facilities can be estimated through a default depth-damage function, which assumes a default building type (i.e., brick for schools, concrete for the other facilities), age (i.e., median), and other characteristics (e.g., first floor elevation, building height, and basement). The default depth-damage function can be adjusted to create a specific curve for the facility under consideration. For detailed information on this, we refer to the technical flood manual issues by FEMA (2013).

4.3 Social vulnerability

Different indicators such as wealth, education, health status, age, gender or ethnicity have been proposed in the literature for characterising social vulnerability (Cutter 2003; Madajewics, 2020). These indicators, or combinations thereof (Koks et al., 2015), can capture the underlying individual and community capacities that determine vulnerability and resilience,

This project has received funding from the European Union's Horizon 2020 research and innovation programme under grant agreement No. 101003598

albeit to variable extent depending on the type of hazard and context (Madajewics, 2020). At the same time, it is important to recognize the spatial variations in the distribution of the vulnerable populations exposed to hazards in order to develop place-based emergency plans (Cutter and Finch., 2008). In this context, spatial indicators of social vulnerability are important for risk management and can be used for the prioritisation of measures (Tate et al., 2021).

Social vulnerability is complex and dynamic, changing not only over space but also through time (Cutter, 2008). However, the evolution of indicators of social vulnerability in time and space is rarely considered in global assessments as information on the relevant parameters is very limited. SSP-based projections for such indicators are available for some countries, usually at sub-national scale or even for continents or regions where the underlying data are available (e.g., Hauer 2019, Terama et al., 2019). Nevertheless, apart from the distribution of Gross Domestic Product (GDP), gridded projections of variables that can be used to assess spatial variations in social vulnerability are generally not available at continental scales. This limits the characterisation of social vulnerability at regional to global scales to simple indicators of exposure of people or assets and does not necessarily reflect the distribution of social vulnerability in space and time.

This project has received funding from the European Union's Horizon 2020 research and innovation programme under grant agreement No. 101003598

5. Procedure for coastal flood risk assessment

Within CoCliCo (Figure 4), coastal flood risk assessments (calculated in WP6) consider the combination of coastal flood and erosion hazards, intensity and likelihood (provided by WP4), exposure, vulnerability and population projections (provided by WP5) to evaluate the adverse consequences of coastal flooding for future climate conditions (based on outcomes of WP3). This common risk calculation procedure complies with IPCC's standards (Abram et al., 2019). In CoCliCo, engagement with Champion users and stakeholder (WP1) will allow ranking user priorities to design and select most relevant risk scenarios to be displayed on the platform – this so-called integrated scenario will guide the production of datasets from WP3 to WP6.

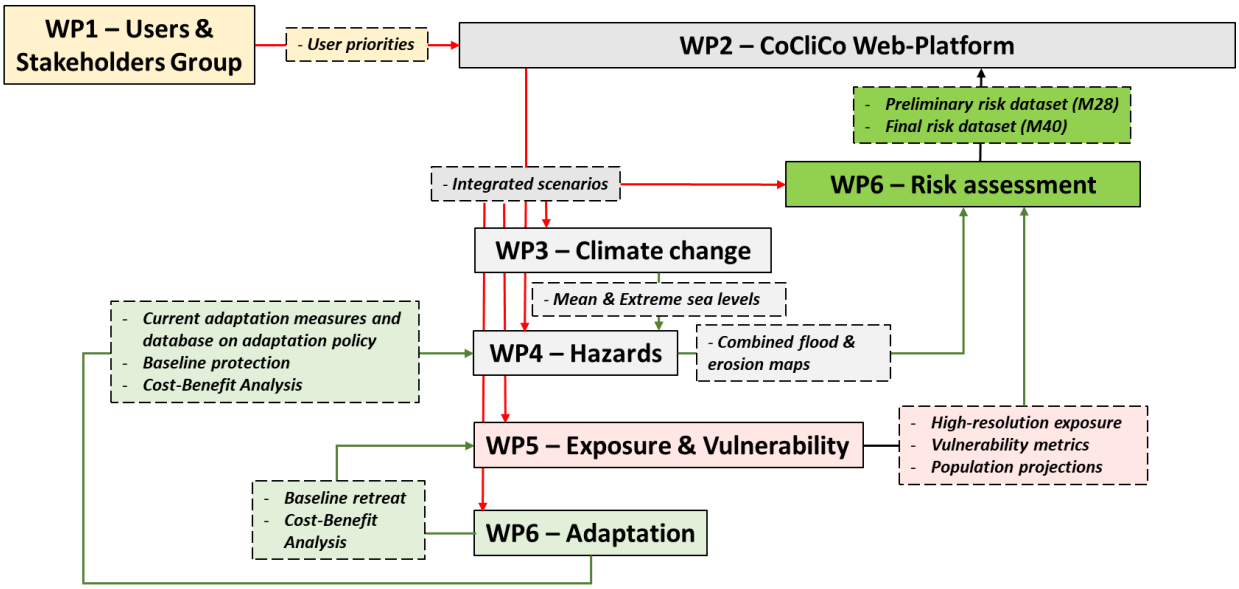

Figure 4. *Workflow of risk assessment designed for CoCliCo. Dotted boxes indicate key dataset/outcomes to be developed and delivered to complete the coastal risk assessment aimed in CoCliCo. Red arrows indicate inputs that originate from the co-design with users/stakeholders (WP1), while green arrows specify key inter-linkages between WP3 to WP6 (risk and adaptation lead science work packages).*

More specifically, integrated scenarios will result in a combination of:

- Climate change scenarios (e.g., RCPs, low/high-end, medium/low confidence, temperature target scenarios), return periods (e.g. 1-in-10 year, 1-in-100 year) for sea levels (WP3) and corresponding flood and erosion hazards layers (WP4).
- Shared Socio-economic pathways (SSPs) for WP5 to define future population, city sprawl, infrastructure and economic assets development.
- Time horizons (e.g., 1990, 2020, 2050, 2100).

This project has received funding from the European Union's Horizon 2020 research and innovation programme under grant agreement No. 101003598

- Adaptation scenarios (e.g., keep flood probability constant in Europe, keep flood disaster costs constant in Europe, cost-efficient adaptation, comparing costs of retreat or accommodation with protection costs) developed in WP6 that will feed back into hazards (WP4) and vulnerability/exposure (WP5).
- "Risk metrics" for WP6 like expected annual population exposure, number of critical infrastructures, expected annual damage, etc. While hazard metrics are essentially value-free, different stakeholders may have different opinions about what exposure or risk metric is most relevant. Therefore, risk metrics are chosen in close collaboration with stakeholders and users in WP1 (in particular user priorities workshop involving the Stakeholder Group, MS1.1, and Decision mapping and associated development priorities, D1.2).

In practice, the calculation will be conducted within the Vigirisk platform[22] as illustrated in Figure 5. This platform will also be used to aggregate the risk metrics for different spatial 'units' (coastal segments, country scale, European scale, etc.), for different assets (population, residential buildings, infrastructures, etc.), and different future climate scenarios (as defined in WP3).

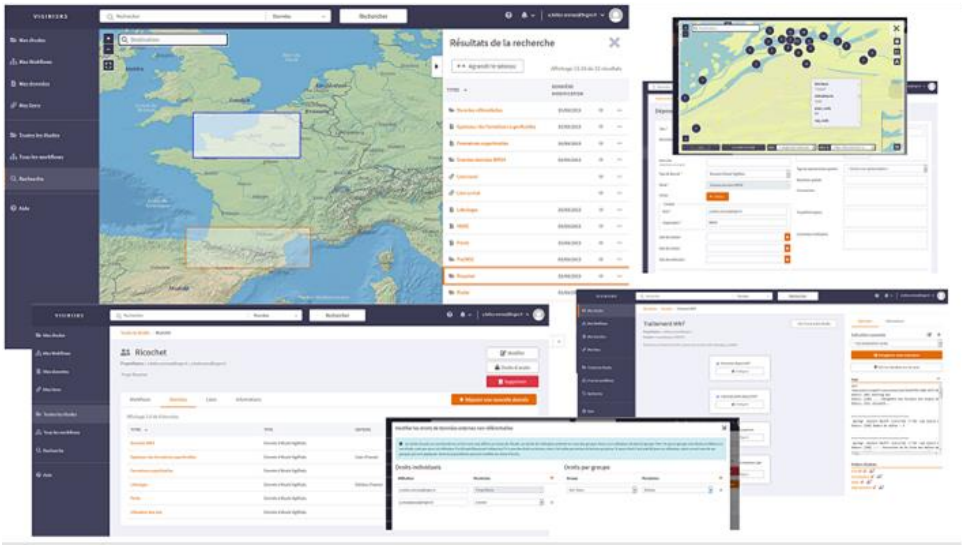

Figure 5. *Vigirisk platform.*

[22] https://www.brgm.fr/en/reference-completed-project/vigirisks-all-one-predictive-platform-natural-risks

This project has received funding from the European Union's Horizon 2020 research and innovation programme under grant agreement No. 101003598

6. Filling data gaps in exposure and vulnerability

This study sets out to improve critical infrastructures' (CIs) exposure to coastal floods by applying Deep Learning (DL) on satellite imagery. Secondly, the vulnerability of CIs will be addressed by using DL for Natural Language Processing to detect infrastructures' service failure from social media and derive vulnerability thresholds.

5.1 Exposure

5.1.1 Objectives

We first aim to fill the gaps in current geospatial exposure databases presented in section 3.2. To accomplish this goal, we aim to develop high-resolution object-based maps of economic assets and infrastructure systems in flood-prone coastal areas. We use satellite imagery in combination with deep learning to automate their detection.

5.1.2 Scientific approach and methodological design

One of the main efforts in Artificial Intelligence (AI) is to solve seemingly intuitive tasks for humans that are hard to formally describe. It is achieved through the ability of DL to gather knowledge from exposing the model to data while avoiding the human operator to formally hard code the knowledge needed. Through a hierarchy of concepts, coining the deep aspect of Deep Learning, the model can learn complicated concepts from simpler ones. For instance, high-level concepts (e.g., a whole object) could be recognised from low-level ones (e.g., corners, edges, colours, and textures) (Goodfellow et al., 2015 p.1-8). These advantages explain the recent rise of DL in satellite imagery analysis by allowing the detection of high-level features without additional data pre-processing (Sun et al., 2019). Another benefit of DL is the equivariance in translation that allows an object to be detected irrespectively to its position in an image. This property allows parameter efficiency and powerful pattern recognition, ultimately yielding to smaller models that are also easier to generalise (Goodfellow et al., 2015, p.1-8).

Three main types of classification tasks can be highlighted while applying AI to computer vision: scene classification, object detection and segmentation. Scene classification aims to determine the category of a whole image (e.g., a forest, an airport, or a beach scene). For that task, the training samples are a series of labelled pictures (Ma et al., 2019). On the other end, object detection aims to detect different objects within a single image (e.g., trees, aeroplanes or people represented in an image). Here, the training samples are pixels confined within a set bounding box fitting the object of interest. Finally, segmentation aims to assign a class to each pixel of an image. Segmentation is subdivided into two types of tasks. In (a) semantic segmentation, pixels of different objects are classified within the same class (Carvalho et al., 2020; Guo et al., 2018). On the other hand, (b) instance segmentation allows differentiating several instances of the same class. This allows to individually separate each object (Carvalho

This project has received funding from the European Union's Horizon 2020 research and innovation programme under grant agreement No. 101003598

et al., 2020). Instance segmentation could thus serve to create a high-resolution map of infrastructures by detecting them at a pixel level while still discerning each object.

The methodology to detect and map infrastructure will follow the eight steps in Figure 6.

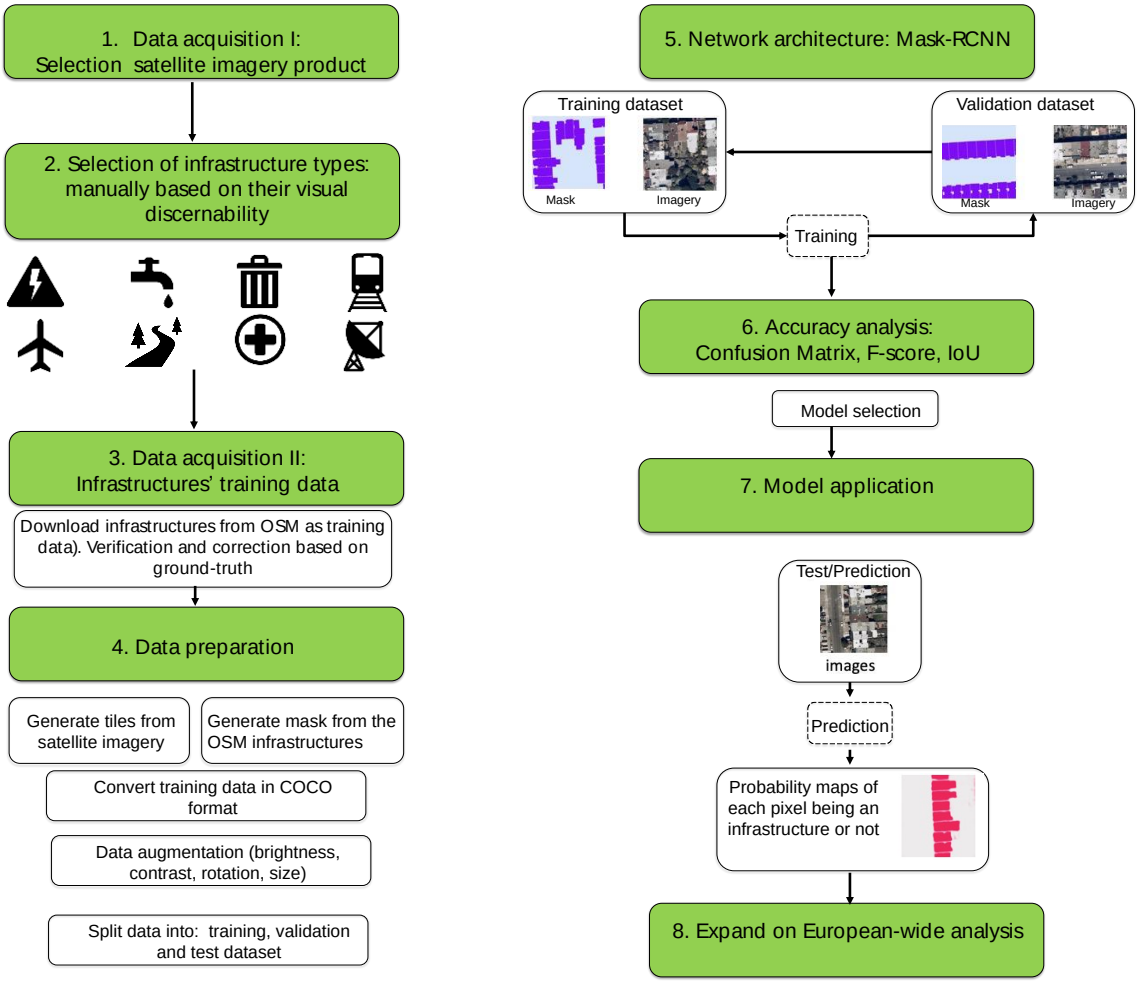

Figure 6. *Methodological design workflow*

Step 1: Data acquisition I: satellite imagery product

First, the selection of the satellite imagery is motivated by the trade-off between high spatial resolution and computation efficiency. On one hand, higher resolution imagery would facilitate the discovery of relevant patterns for the DL model. However, it would also overcomplicate the model and lead to more computer-intensive training and applications of the models. To guarantee the visibility of the infrastructures, we therefore settle for a resolution of 1.5 meters.

This project has received funding from the European Union's Horizon 2020 research and innovation programme under grant agreement No. 101003598

The first test will focus on detecting infrastructures within the Netherlands using the Netherlands Space Office product[23]. This will allow having readily accessible imagery product to initiate the research and to simultaneously start the request procedure for the SPOT 6 and 7 to European Space Agency. The SPOT imagery will consist of cloud processed 1.5 m resolution 4-bands pan-sharpened .geoTIFF raster.

Step 2: Selection of infrastructure types

The first task to understand which infrastructure could be extracted using DL will be to test the discernability of the infrastructures. The initial focus will be on the energy sector's critical infrastructures (Table 3). Test models for the Netherlands will be created to decide which infrastructure types are detectable. Furthermore, this step would allow to test if the resolution used is sufficiently fine. This implies that a model for each subtype of energy infrastructure should be created.

Table 3. *List of infrastructure types within the energy system.*

System	Subsystem	Infrastructure type
Energy	Power	cable
		line
		minor line
		plant
		substation
		power tower
		power pole

Step 3: Data acquisition II: Infrastructures' training data

The DL models are learnt through exposing them to training data. Compared to traditional Machine Learning models, DL requires a larger amount of training data because the features are not selected by the human but are learnt through optimisation from the training data. It is thus paramount to acquire sufficient training data representing the diversity of infrastructures found within the research area. However, annotated datasets for remote sensing applications are still lacking (Ayala et al., 2021; Carvalho et al., 2020). Therefore, infrastructures from OSM

[23] https://www.spaceoffice.nl/en/satellite-data-portal/

This project has received funding from the European Union's Horizon 2020 research and innovation programme under grant agreement No. 101003598

will be extracted at a national level using the publicly available code OSM clipper[24] in a .PBF format following the attribute tags (keys and values) found in Nirandjan et al. (in press). The OSM object will then be converted into a vector layer in a. GPKG format.

Some challenges are inevitable to using OSM for training data, most notably omission (i.e., unregistered objects) and registration noises (i.e., inaccurate registration) (Ayala et al., 2021; Senaratne et al., 2017). Therefore, OSM objects will be manually verified to make sure of their alignment and truthfulness to the ground-truth satellite imagery. Also, national databases will be consulted to complete potential omissions in OSM. The polygons representing the infrastructures will be adjusted using QGIS[25].

Step 4: Training data preparation

Training data labelling and segmentation mask
The training data labelling in instance segmentation requires both a segmentation mask at a pixel level and a polygon delimitating the object within its bounding box. For the segmentation mask, the polygons representing the infrastructures retrieved from OSM will be used to create a mask layer, with the polygons labelled as 1. The background, or the absence of infrastructure, is labelled as 0. The training data will also be adapted to the Creating Common Object in Context (COCO) labelling format in .JSON format (Fleet et al., 2014).

Splitting the training datasets into tiles
Satellite imagery comes in large size in comparison to traditional Red-Green and Blue (RGB) images. Thus, the input must be divided into tiles or patches of a manageable size. This also requires a sliding window with a predefined stride value to establish an overlap interval between the tiles (Ayala et al., 2021; Carvalho et al., 2020; Yi et al., 2019). Both the sliding window and stride should be set to allow to capture the context of the image (Carvalho et al., 2020; de Albuquerque et al., 2020).

Data augmentation
The data augmentation of the training dataset aims to avoid overfitting and enhance the models' ability to learn new features by including variations in the rotation, brightness, contrast and size of the objects.

Splitting training dataset into training, validation, and test set
The training dataset will be divided into three parts: (a) training, (b) validation and (c) test set. The training dataset will be used to learn the model. The validation set will be used to evaluate the models and tune the hyperparameters (batch size, number of epochs, learning rate, etc.). The test set will only be used at the end of that process to accurately evaluate the model's performance.

Step 5: Network architecture
The state-of-the-art architecture for instance segmentation is currently Mask-RCNN. A framework introduced by Facebook Artificial Intelligence Research (FAIR) (He et al., 2017). It

[24] Koks, E. (2022, February 22) OSM Clipper [https://github.com/ElcoK/osm_clipper]

[25] QGIS (2022, February 22) [https://www.qgis.org/en/site/]

This project has received funding from the European Union's Horizon 2020 research and innovation programme under grant agreement No. 101003598

has been applied in several successful cases to satellite imagery analysis (Carvalho et al., 2020; de Albuquerque et al., 2020).

Step 6: Accuracy analysis
The accuracy of the models will be based on the Confusion Matrix (Table 4) and Intersection over Union (IoU), from which the Precision and Recall will be calculated.

Table 1. Confusion matrix

		Predicted condition	
		Positive	***Negative***
Observed conditions	***True***	True Positives	False Negatives
	False	False Positives	True Negatives

$$Intersection\ over\ Union = \frac{Area\ of\ Overlap}{Area\ of\ Union}$$

$$Precison = \frac{True\ Positives}{(True\ Posotives + False\ Positives}$$

$$Recall = \frac{True\ Positives}{(True\ Positives + False\ Negatives)}$$

Step 7: Model application
The model will then be applied on new satellite imagery that has not been used during the training to detect infrastructures.

Step 8: Expand on European-wide analysis
Following the test at the Netherlands scale, the training data and application will be expanded to an EU-wide scale.

5.2 Vulnerability

5.2.1 Objectives

Flood risk is a function of hazard, exposure, and vulnerability, here defined as the capacity of a society to deal with a flood event (IPCC, 2012; Koks et al., 2015; Kron, 2005). In the literature, the vulnerability of the built environment is commonly determined using depth damage or fragility curves. Those curves provide insights into the damages that occur at a

This project has received funding from the European Union's Horizon 2020 research and innovation programme under grant agreement No. 101003598

specific water depth for each category of land-use (e.g., residential building, commerce, industry transport, infrastructure and agriculture) (Huizinga et al., 2017).

However, the analysis of infrastructure's vulnerability is hampered by the lack of sources on their vulnerability due to the information confidentiality imposed by security and competition concerns (Huizinga et al., 2017). More importantly, economic damages capture only part of the impact of floods. In the case of critical infrastructures, vulnerability should also encompass their ability to deliver their vital services to society during a flood event and their ability to recover from such disruption (i.e., resilience) (Serre et al., 2016).

Hence, this study first seeks to first determine service failure thresholds of critical infrastructures in response to flood intensity, and secondly, to determine their resilience by monitoring the delay to recover from flood-induced disruptions.

5.1.2 Scientific approach and methodological design

Over the past decade social media gained traction as a relevant source of information to monitor natural hazards from an impact perspective (Avvenuti et al., 2014; Gupta et al., 2013; Wang et al., 2016; Wang & Ye, 2018). Among its benefits, social media provide high temporal resolution, allowing to analyse their response during disasters (Blanford et al., 2014). For this study, a social media analysis will be performed to determine the services failure threshold of CIs in relation to flood depth. The platform Twitter will be used for its ease of access through its API and its availability for research (Twitter, 2021).

First, areas that experiences historic flood events will be selected in regions presenting a high Twitter penetration rate. Then, tweets from utilities' accounts will be scraped to detect the onset of service failure. To determine the resilience of the infrastructure system, tweets in the affected area will be monitored to determine the length of the disturbance (in .JSON format). To limit the number of tweets to download, tweets presenting mentions of a flood event, infrastructure failures or locations of the event will be downloaded. The location will be determined using the automatically attached GPS location. However, since geolocated tweets only represent a small fraction of the total amount of published tweets (de Bruin et al., 2018), a Named-Entity Recognition (NER) analysis of the tweets' content using the Python module spaCy[26] will be done to detect mentions of location and match the location to the Nominatim[27] database to determine the coordinates of the tweets.

The downloaded tweets will partly be used to train a binary DL model aimed at detecting service disruption. Tweets referencing a service failure will be labelled as 1, while the other will be labelled as 0. After the validation and testing of the model, it will be used to correctly classify tweets mentioning service failure during past flood events.

The method to build the neural network for the natural language processing will take advantage of the multi-lingual LASER sentence embedding (Language-Agnostic Sentence

[26] spaCy (2022, February 22) [https://spacy.io/]

[27] Nominatim (2022, February, 22) [https://nominatim.org/]

This project has received funding from the European Union's Horizon 2020 research and innovation programme under grant agreement No. 101003598

Representations) from Meta AI. Embeddings are vector representations of sentences. This allows to map semantical similar sentences close to each other. This method unlocks the possibility to train a model in one language while still being able to deploy it in more than 100 other languages that have not been used during the training (Figure 7).

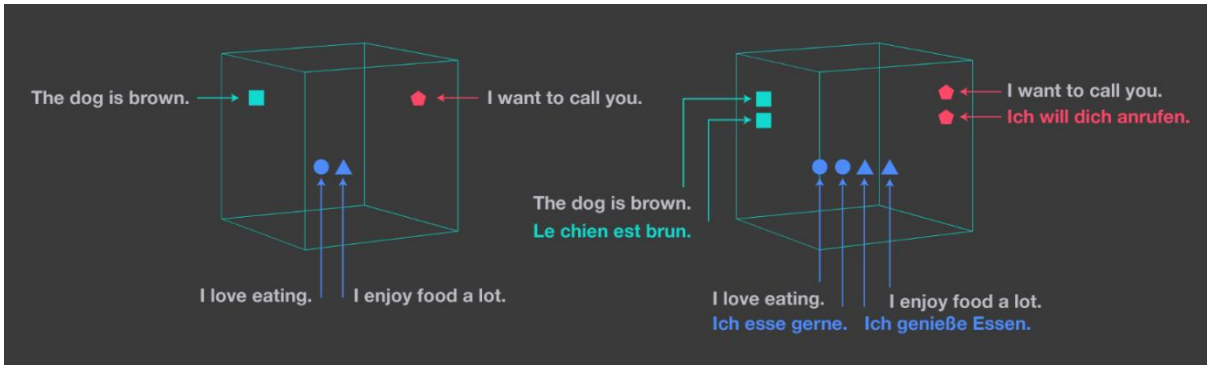

Figure 7. *Representation of mono-lingual (left) and the LASER multi-lingual embeddings (right) (Facebook AI, 2019).*

This project has received funding from the European Union's Horizon 2020 research and innovation programme under grant agreement No. 101003598

7. Adaptation

The state of the art in adaptation modelling is modelling of hard defences, e.g., dikes (Hinkel et al., 2014; Vousdoukas et al., 2016, 2020a, Prahl et al. 2018, Diaz 2016). Attempts behind this modelling have been undertaken through, for instance, the modelling of beach nourishment as adaptation to erosion (Hinkel et al 2013) and in the modelling of river mouth barriers (Nicholls et al, 2019). Retreat has been analysed in the form of setback zones (Lincke et al, 2020) and large-scale coastal migration (Lincke and Hinkel, 2021). The potential of nature-based solutions is still subject to extensive research, with some first indications of the attenuation being available (Vafeidis et al., 2019). Attempts to model accommodation have been undertaken in the COACCH project (COACCH 2021). Integrated adaptation assessments are still rare, but retreat and protection have been combined (Diaz 2016, Lincke and Hinkel 2021) and accommodation and protection have at least been compared (COACCH 2021).

Data on adaptation is still rare. Adaptation unit cost is usually taken from the few empirical studies (Jonkman et al., 2013) or updates from this (Nicholls, 2019). Data on existing protection is one of the major sources of uncertainty, which is supposed to be closed in CoCliCo. The state of the art is either to model existing protection, either via a demand-for-safety function (Hinkel et al. 2014), or via expert judgement (Sadoff et al., 2015, Hallegatte et al., 2013), or via existing databases like FLOPROS (Scussolini, 2016) - where the latter itself is obtained from a multi-layer model (including expert judgement). Existing adaptation policies are not known except from a very few countries such as Germany, the UK and the Netherlands (Bisaro et al., 2020). In WP6 of CoCliCo this gap will be closed at least on European level by building a GIS layer of existing protection infrastructure and a database of existing national adaptation policies. While the layer of existing protection infrastructure will feed directly in the risk layers, the database of existing national adaptation policies will be used to develop baseline adaptation scenarios. Existing policies and observed existing adaptations will be stylized into simple empirical models and associated investment and maintenance unit cost functions. These stylized models will be mapped to the coastal Flood Risk Management Units developed in CoCliCo (see below) and used to model future adaptation.

Assessing coastal adaptation measures also requires appropriate spatial units. While for impact and risk assessment grid cells or objects might be appropriate spatial units, this is not the case for adaptation modelling. For instance, a grid cell in the middle of a small island might be flooded from different directions and so protection of the grid cell might involve protection infrastructure at more than one site. State of the art spatial unit are coastline segments (Vafeidis et al., 2008) the segment the coastline into pieces with homogenous characteristics but heterogenous length. However, this does not solve the issues stated above as areas can only be assigned to one segment. In CoCliCo this issue will be addressed by the introduction of flood risk management units for Europe. This automated process will work with existing datasets and the datasets produced in the project (datasets of mean and extreme sea-level

This project has received funding from the European Union's Horizon 2020 research and innovation programme under grant agreement No. 101003598

from WP3, the identified coastal flood plains in WP4, and the initial exposure and vulnerability maps from WP5. The segmentation will produce a set of floodplains and connected coastline segments (which form a network as one flood plain might be connected to several segments).

This project has received funding from the European Union's Horizon 2020 research and innovation programme under grant agreement No. 101003598

8. Concluding remarks and moving forward

This report has presented an overview of the current state-of-knowledge on exposure, vulnerability, risk and adaptation in relation to the built environment. While the report has shown that there is a wealth of knowledge and data available at the start of this project, several gaps have been identified that need and will be addressed within CoCliCo:

- Identify and fill the gaps in geospatial data of critical infrastructure assets. While some infrastructure assets may have a good coverage of data availability across Europe through open-source initiatives such as OpenStreetMap (e.g., transport infrastructure), several infrastructures are also still far from complete (e.g., low-tier electricity networks).
- A lack of knowledge on future developments of population exposure under different scenarios. This is true not only for economic scenarios, but also adaptation scenarios. How will adaptation measures influence the development of population? Within CoCliCo, we hope to provide first answers.
- While much work has been done already on the identification of physical vulnerability of (infrastructure) assets to flooding, little is still known about the impact of flooding to network service reliability and functioning. Within CoCliCo, we will make first steps in using social media and novel Natural Language Processing methods to develop a first set of vulnerability thresholds to provide a link between hazard intensity and network service functioning.
- Finally, CoCliCo will make additional steps in developing a wide range of coastal adaptation measures for Europe, ranging from nature-based solutions to coastal migration. These measures will be incorporated within a risk modelling framework, allowing us to assess the potential benefits of each individual measure.

Next to providing a starting point for the work to be done in CoCliCo, this report also identified a major shortcoming within European data provision: there is a clear lack of standardized infrastructure data across Europe. While open-source data such as OpenStreetMap partly fills this gap (also within CoCliCo), an EU-centralized approach to develop a geospatial database of critical infrastructure assets would be a much-needed step in improving such risk assessments.

This project has received funding from the European Union's Horizon 2020 research and innovation programme under grant agreement No. 101003598

9. References

Abram, N., Gattuso, J. P., Prakash, A., Cheng, L., Chidichimo, M. P., Crate, S., ... & Von Schuckmann, K. (2019). Framing and context of the report. *IPCC special report on the ocean and cryosphere in a changing climate*, 73-129.

André, C., Monfort, D., Bouzit, M., & Vinchon, C. (2013). Contribution of insurance data to cost assessment of coastal flood damage to residential buildings: insights gained from Johanna (2008) and Xynthia (2010) storm events. *Natural Hazards and Earth System Sciences*, *13*(8), 2003-2012.

Ayala, C., Sesma, R., Aranda, C., & Galar, M. (2021). A Deep Learning Approach to an Enhanced Building Footprint and Road Detection in High-Resolution Satellite Imagery. *Remote Sensing*, *13*(16), 3135. https://doi.org/10.3390/rs13163135

Bensi, M., Ferrante, F. and Philip, J. (2015). Assessment of Flood Fragility for Nuclear Power Plants: Challenges and Next Steps.

Bisaro, A., de Bel, M., Hinkel, J., Kok, S., Stojanovic, T., Ware, D. (2020). Multilevel governance of coastal flood risk reduction: A public finance perspective. Environmental Science & Policy 112, 203-212. https://doi.org/10.1016/j.envsci.2020.05.018

Blanford, J. I., Bernhardt, J., Savelyev, A., Wong-Parodi, G., Carleton, A. M., Titley, D. W., & MacEachren, A. M. (2014, May). Tweeting and tornadoes. In *ISCRAM*.

Bensi, M., Ferrante, F. and Philip, J. (2015). Assessment of Flood Fragility for Nuclear Power Plants: Challenges and Next Steps.

Burns & McDonnel (n.d). Impacts on Underground Transmission Assets due to Flooding Caused by Major.

Büttner, G. (2014). CORINE land cover and land cover change products. In Land use and land cover mapping in Europe (pp. 55-74). Springer, Dordrecht.

Carvalho, O. L. F. de, de Carvalho Júnior, O. A., Albuquerque, A. O. de, Bem, P. P. de, Silva, C. R., Ferreira, P. H. G., Moura, R. dos S. de, Gomes, R. A. T., Guimarães, R. F., & Borges, D. L. (2020). Instance Segmentation for Large, Multi-Channel Remote Sensing Imagery Using Mask-RCNN and a Mosaicking Approach. *Remote Sensing*, *13*(1), 39. https://doi.org/10.3390/rs13010039

COACCH (2021). Deliverable 4.2 Sectoral assessments of policy effectiveness.

Cutter, S. L., Boruff, B. J., & Shirley, W. L. (2003). Social vulnerability to environmental hazards. Social science quarterly, 84(2), 242-261.

Cutter, S.L. (2003). The vulnerability of science and the science of vulnerability. Annals of the Association of American Geographers, 93(1), pp.1-12.

Cutter, S. L., and Finch, C. (2008). Temporal and spatial changes in social vulnerability to natural hazards. Proceedings of the national academy of sciences, 105(7), 2301-2306.

This project has received funding from the European Union's Horizon 2020 research and innovation programme under grant agreement No. 101003598

Diaz, D.B. Estimating global damages from sea level rise with the Coastal Impact and Adaptation Model (CIAM). *Climatic Change* **137,** 143–156 (2016). https://doi.org/10.1007/s10584-016-1675-4

Diaz Loaiza, M. A., Bricker, J. D., Meynadier, R., Duong, T., Ranasinghe, R., & Jonkman, S. (2021). Development of damage curves for buildings near La Rochelle during Storm Xynthia based on insurance claims and hydrodynamic simulations. *Natural Hazards and Earth System Sciences Discussions*, 1-18.

European Commission (2021). Technical guidance on the climate proofing of infrastructure in the period 2021-2027. EC 2021/C 373/01

Facebook AI (2019, January 22). Zero-shot transfer across 93 languages: Open-sourcing enhanced LASER library. Meta AI. https://ai.facebook.com/blog/laser-multilingual-sentence-embeddings/

Fekete, A. (2009). Validation of a social vulnerability index in context to river-floods in Germany. Natural Hazards and Earth System Sciences, 9(2), 393-403.

FEMA (2013). Hazus-MH Technical Manual Flood Model, Washingt. D.C Dep. Homel. Secur. FEMA (2021). Hazus Inventory Technical Manual, 185.

Forzieri, G., Bianchi, A., e Silva, F. B., Herrera, M. A. M., Leblois, A., Lavalle, C., ... & Feyen, L. (2018). Escalating impacts of climate extremes on critical infrastructures in Europe. Global environmental change, 48, 97-107.

Fleet, D., Pajdla, T., Schiele, B., & Tuytelaars, T. (Eds.). (2014). *Computer Vision – ECCV 2014: 13th European Conference, Zurich, Switzerland, September 6-12, 2014, Proceedings, Part V* (Vol. 8693). Springer International Publishing. https://doi.org/10.1007/978-3-319-10602-1

van Ginkel, K. C. H., Dottori, F., Alfieri, L., Feyen, L. and Koks, E. E.: Flood risk assessment of the European road network, Nat. Hazards Earth Syst. Sci., 21(3), 1011–1027, doi:10.5194/nhess-21-1011-2021, 2021.

Goodfellow, I., Bengio, Y., & Courville, A. (2016). Chapter 1. *Deep learning*. MIT press.

Guo, Y., Liu, Y., Georgiou, T., & Lew, M. S. (2018). A review of semantic segmentation using deep neural networks. *International Journal of Multimedia Information Retrieval*, *7*(2), 87–93. https://doi.org/10.1007/s13735-017-0141-z

Hallegatte, S., Rentschler, J., & Rozenberg, J. (2019). Lifelines: The resilient infrastructure opportunity. World Bank Publications.

Hallegatte, S., Green, C., Nicholls, R.J., Corfee-Morlot, J. (2013) Future flood losses in major coastal cities. Nature Climate Change 3, 802–806 https://doi.org/10.1038/nclimate1979

Hall, J. W., Thacker, S., Ives, M. C., Cao, Y., Chaudry, M., Blainey, S. P., & Oughton, E. J. (2016, November). Strategic analysis of the future of national infrastructure. In Proceedings of the Institution of Civil Engineers-Civil Engineering (Vol. 170, No. 1, pp. 39-47). Thomas Telford Ltd.

This project has received funding from the European Union's Horizon 2020 research and innovation programme under grant agreement No. 101003598

Hall, K. L.: Out of Sight , Out of Mind Revisited An Updated Study on the Undergrounding Of Overhead Power Lines, Undergr. Constr., (December), 2009.

Hauer, M. E. (2019). Population projections for US counties by age, sex, and race controlled to shared socioeconomic pathway. Scientific data, 6(1), 1-15.

He, K., Gkioxari, G., Dollár, P., & Girshick, R. (2017). Mask R-CNN. *2017 IEEE International Conference on Computer Vision (ICCV)*, 2980–2988. https://doi.org/10.1109/ICCV.2017.322

Hinkel, J., Nicholls, R.J., Tol, R., Wang, Z. B., Hamilton, J., Boot, G., Vafeidis, A., Mcfadden, L., Ganopolski, A., Klein, R. (2013). A global analysis of erosion of sandy beaches and sea-level rise: An application of DIVA. Global and Planetary Change. 111. 150-158. https://doi.org/10.1016/j.gloplacha.2013.09.002

Hinkel, J., D. Lincke, A. T. Vafeidis, M. Perrette, R. J. Nicholls, R. S. J. Tol, B. Marzeion, X. Fettweis, C. Ionescu, and A. Levermann (2014). Coastal flood damage and adaptation cost under 21st century sea-level rise. Proceedings of the National Academy of Sciences 111 (9), p. 3292–3297. https://doi.org/10.1073/pnas.1222469111 1222469111.

Huizinga, H. J.: Flood damage functions for EU member states, Lelystad, the Netherlands., 2007.

Huizinga, J., de Moel, H. and Szewczyk, W.: Global flood depth-damage functions: Methodology and the Database with Guidelines., 2017.

IPCC (2012). *Managing the Risks of Extreme Events and Disasters to Advance Climate Change Adaptation: Special Report of the Intergovernmental Panel on Climate Change*. Cambridge University Press.

Jones, B., and O'Neill, B. C. (2016). Spatially explicit global population scenarios consistent with the Shared Socioeconomic Pathways. Environmental Research Letters, 11(8), 084003.

Jongman, B., Kreibich, H., Apel, H., Barredo, J. I., Bates, P. D., Feyen, L., Gericke, A., Neal, J., Aerts, J. C. J. H. and Ward, P. J.: Comparative flood damage model assessment: Towards a European approach, Nat. Hazards Earth Syst. Sci., 12(12), 3733–3752, doi:10.5194/nhess-12-3733-2012, 2012.

Jonkman, S.N., Hillen, M.M., Nicholls, R.J., Kanning, W., van Ledden, M., 2013. Costs of Adapting Coastal Defences to Sea-Level Rise— New Estimates and Their Implications. Journal of Coastal Research 1212–1226. https://doi.org/10.2112/JCOASTRES-D-12-00230.1

Gil, J., & Steinbach, P. (2008). From flood risk to indirect flood impact: evaluation of street network performance for effective management, response and repair. WIT Transactions on Ecology and the Environment, 118, 335-344.

Kellermann, P., Schöbel, A., Kundela, G. and Thieken, A. H.: Estimating flood damage to railway infrastructure - The case study of the March River flood in 2006 at the Austrian Northern Railway, Nat. Hazards Earth Syst. Sci., 15(11), 2485–2496, doi:10.5194/nhess-15-2485-2015, 2015.

This project has received funding from the European Union's Horizon 2020 research and innovation programme under grant agreement No. 101003598

Kim, B. J., Kim, M., Hahm, D., Park, J. and Han, K. Y.: Probabilistic flood assessment methodology for nuclear power plants considering extreme rainfall, Energies, 14(9), 1–27, doi:10.3390/en14092600, 2021.

Kok, M., Huizinga, H. J. and Barendregt, A. (2005). Standard Method 2004: Damage and Casualties Caused by Flooding.

Koks, E. E., Jongman, B., Husby, T. G., & Botzen, W. J. W. (2015). Combining hazard, exposure and social vulnerability to provide lessons for flood risk management. *Environmental Science & Policy*, *47*, 42–52. https://doi.org/10.1016/j.envsci.2014.10.013

Koks, E. E., Ginkel, K. C. H. Van, Marle, M. J. E. Van and Lemnitzer, A. (2021) Brief Communication : Critical Infrastructure impacts of the 2021 mid- July western European flood event, (December), 1–11, doi:10.5194/nhess-9-1679-2009

Koks, E. E., & Haer, T. (2020). A high-resolution wind damage model for Europe. Scientific reports, 10(1), 6866.

Koks, E. E., Rozenberg, J., Zorn, C., Tariverdi, M., Vousdoukas, M., Fraser, S. A., ... & Hallegatte, S. (2019). A global multi-hazard risk analysis of road and railway infrastructure assets. Nature communications, 10(1), 1-11.

Kreibich, H., Piroth, K., Seifert, I., Maiwald, H., Kunert, U., Schwarz, J., Merz, B. and Thieken, A. H.: Is flow velocity a significant parameter in flood damage modelling?, Nat. Hazards Earth Syst. Sci., 9(5), 1679–1692, doi:10.5194/nhess-9-1679-2009, 2009.

Kulp, S. A., and Strauss, B. H. (2019). New elevation data triple estimates of global vulnerability to sea-level rise and coastal flooding. Nature communications, 10(1), 1-12.

Leyk, S., Gaughan, A. E., Adamo, S. B., de Sherbinin, A., Balk, D., Freire, S., ... & Pesaresi, M. (2019). The spatial allocation of population: a review of large-scale gridded population data products and their fitness for use. Earth System Science Data, 11(3), 1385-1409.

Lincke, D., Hinkel, J. (2021). Coastal migration due to 21st century sea- level rise. *Earth's Future*, 9, e2020EF001965. https://doi.org/10.1029/2020EF001965

Lincke, D., Wolff, C., Hinkel, J., Vafeidis, A.T., Blickensdörfer, L., Povh Skugor, D. (2020). The effectiveness of setback zones for adapting to sea-level rise in Croatia. *Regional Environmental Change* 20(46). https://doi.org/10.1007/s10113-020-01628-3

Ma, L., Liu, Y., Zhang, X., Ye, Y., Yin, G., & Johnson, B. A. (2019). Deep learning in remote sensing applications: A meta-analysis and review. *ISPRS Journal of Photogrammetry and Remote Sensing*, *152*, 166–177. https://doi.org/10.1016/j.isprsjprs.2019.04.015

Madajewicz, M. (2020). Who is vulnerable and who is resilient to coastal flooding? Lessons from Hurricane Sandy in New York City. Climatic Change, 163(4), 2029-2053.

Merkens, J. L., Reimann, L., Hinkel, J., & Vafeidis, A. T. (2016). Gridded population projections for the coastal zone under the Shared Socioeconomic Pathways. Global and Planetary Change, 145, 57-66.

This project has received funding from the European Union's Horizon 2020 research and innovation programme under grant agreement No. 101003598

Merkens, J. L., Lincke, D., Hinkel, J., Brown, S., & Vafeidis, A. T. (2018). Regionalisation of population growth projections in coastal exposure analysis. Climatic Change, 151(3), 413-426.

Merz, B., Kreibich, H., Schwarze, R., & Thieken, A. (2010). Review article" Assessment of economic flood damage". Natural Hazards and Earth System Sciences, 10(8), 1697-1724.

Miyamoto International: INCREASING INFRASTRUCTURE RESILIENCE BACKGROUND REPORT, World Bank, Washington, DC., 2019.

Nicholls,R.J., Hinkel, J., Lincke, D., van der Pol, T. (2019). Global Investment Costs for Coastal Defense through the 21st Century. The World Bank Policy Research Working Paper Series 8745, https://ideas.repec.org/p/wbk/wbrwps/8745.html.

Nirandjan, S., Koks, E.E., Ward, P.J. & Aerts, C.J.H. (in press). A spatially-explicit harmonized global dataset of critical infrastructure. Scientific Data.

Nirandjan, S., Koks, E.E., Van Ginkel, K.C.H., Aerts, C.J.H. & Ward, P.J. (in progress). Physical vulnerability database for critical infrastructure multi-hazard risk assessments - a systematic review and data collection. Nat. Hazards Earth Syst. Sci.

O'Neill, B.C., Kriegler, E., Riahi, K., Ebi, K.L., Hallegatte, S., Carter, T.R., Mathur, R. and van Vuuren, D.P., 2014. A new scenario framework for climate change research: the concept of shared socioeconomic pathways. Climatic change, 122(3), pp.387-400.

Oppenheimer, M., Glavovic, B., Hinkel, J., van de Wal, R., Magnan, A. K., Abd-Elgawad, A., et al. (2019). Sea level rise and implications for low lying islands, coasts and communities. In Special report on the ocean and cryosphere in a changing climate. Oxford University Press.

Prahl, B. F., Boettle, M., Costa, L., Kropp, J. P., & Rybski, D. (2018). Damage and protection cost curves for coastal floods within the 600 largest European cities. Scientific Data, 5, 180034. https://doi.org/10.1038/sdata.2018.34

Senaratne, H., Mobasheri, A., Ali, A. L., Capineri, C., & Haklay, M. (Muki). (2017). A review of volunteered geographic information quality assessment methods. *International Journal of*

Rasmussen, D. J., Kopp, R. E., Kulp, S. A., Oppenheimer, M., & Strauss, B. (2020, December). Physical extreme sea level metrics may misrepresent future flood risk. In *AGU Fall Meeting 2020*. AGU.

Reimann, L., Merkens, J. L., & Vafeidis, A. T. (2018). Regionalized Shared Socioeconomic Pathways: narratives and spatial population projections for the Mediterranean coastal zone. Regional Environmental Change, 18(1), 235-245.

Rosina, K., e Silva, F. B., Vizcaino, P., Herrera, M. M., Freire, S., & Schiavina, M. (2018). Increasing the detail of European land use/cover data by combining heterogeneous data sets. International Journal of Digital Earth.

Sadoff, C.W., Hall, J.W., Grey, J.C.J.H., D. an. Aerts, Ait-Kadi, M., Brown, C., Cox, A., Dadson, S., Garrick, D., Kelman, J., McCornick, P., Ringler, C., Rosegrant, M., Whittington, D., Wiberg,

This project has received funding from the European Union's Horizon 2020 research and innovation programme under grant agreement No. 101003598

D., 2015. Securing Water, Sustaining Growth: Report of the GWP/OECD Task Force on Water Security and Sustainable Growth.

Senaratne, H., Mobasheri, A., Loai Ali, A., Capineri, C., & (Muki) Haklay, M. (2017) A review of volunteered geographic information quality assessment methods, International Journal of Geographical Information Science, 31:1, 139-167, doi: 10.1080/13658816.2016.1189556

Scussolini, P., Aerts, J. C. J. H., Jongman, B., Bouwer, L. M., Winsemius, H. C., de Moel, H., and Ward, P. J. (2016): FLOPROS: an evolving global database of flood protection standards, Nat. Hazards Earth Syst. Sci., 16, 1049–1061, https://doi.org/10.5194/nhess-16-1049-2016

Serre, D. (2016). Advanced methodology for risk and vulnerability assessment of interdependency of critical infrastructure in respect to urban floods. *E3S Web of Conferences*, *7*, 07002. https://doi.org/10.1051/e3sconf/20160707002

Sun, G., Huang, H., Zhang, A., Li, F., Zhao, H., & Fu, H. (2019). Fusion of Multiscale Convolutional Neural Networks for Building Extraction in Very High-Resolution Images. *Remote Sensing*, *11*(3), 227. https://doi.org/10.3390/rs11030227

Tate, E., Rahman, M. A., Emrich, C. T., and Sampson, C. C. (2021). Flood exposure and social vulnerability in the United States. Natural Hazards, 106(1), 435-457.

Terama, E., Clarke, E., Rounsevell, M. D., Fronzek, S., and Carter, T. R. (2019). Modelling population structure in the context of urban land use change in Europe. Regional environmental change, 19(3), 667-677.

Tiggeloven, T., De Moel, H., Winsemius, H. C., Eilander, D., Erkens, G., Gebremedhin, E., ... and Ward, P. J. (2020). Global-scale benefit–cost analysis of coastal flood adaptation to different flood risk drivers using structural measures. Natural Hazards and Earth System Sciences, 20(4), 1025-1044.

Vafeidis, A. T., Nicholls, R. J., McFadden, L., Tol, R. S. J., Hinkel, J., Spencer, T., Grashoff, P. S., Boot, G., & Klein, R. J. T. (2008). A New Global Coastal Database for Impact and Vulnerability Analysis to Sea-Level Rise. *Journal of Coastal Research*, *24*(4), 917–924. http://www.jstor.org/stable/40065185

Vafeidis, A.T., Schuerch, M., Wolff, C., Spencer, T., Merkens, J.L., Hinkel, J., Lincke, D., Brown, S., Nicholls, R.J. (2019). Water-level attenuation in global-scale assessments of exposure to coastal flooding: a sensitivity analysis. *Natural Hazards and Earth Systen Science*, 19, p. 973-984. https://doi.org/10.5194/nhess-19-973-2019

Vousdoukas, M. I., Mentaschi, L., Voukouvalas, E., Bianchi, A., Dottori, F., & Feyen, L. (2018). Climatic and socioeconomic controls of future coastal flood risk in Europe. *Nature Climate Change*, *8*(9), 776-780.

Wang, Z., & Ye, X. (2018). Social media analytics for natural disaster management. *International Journal of Geographical Information Science*, *32*(1), 49–72. http://doi.org/10.1080/13658816.2017.1367003

Wing, O. E., Lehman, W., Bates, P. D., Sampson, C. C., Quinn, N., Smith, A. M., ... & Kousky, C. (2022). Inequitable patterns of US flood risk in the Anthropocene. *Nature Climate Change*, 1-7.

This project has received funding from the European Union's Horizon 2020 research and innovation programme under grant agreement No. 101003598

Wolff, C. (2020). Addressing data limitations and uncertainties in broad-scale coastal flood-risk assessments. PhD Thesis, Universitätsbibliothek Kiel.

Wolfgang, K. (2005). Flood Risk= Hazard. Values. Vulnerability. *Water International*, *30*(1), 58-68.

Yi, Y., Zhang, Z., Zhang, W., Zhang, C., Li, W., & Zhao, T. (2019). Semantic Segmentation of Urban Buildings from VHR Remote Sensing Imagery Using a Deep Convolutional Neural Network. *Remote Sensing*, *11*(15), 1774. https://doi.org/10.3390/rs11151774

This project has received funding from the European Union's Horizon 2020 research and innovation programme under grant agreement No. 101003598